Octet and decuplet baryons in a covariant and confining diquark-quark model

M. Oettel,* G. Hellstern,† R. Alkofer,‡ and H. Reinhardt

Institute for Theoretical Physics, Tübingen University, Auf der Morgenstelle 14, D–72076 Tübingen, Germany

(Received 29 May 1998)

The baryon octet and decuplet masses and Bethe-Salpeter vertex and wave functions are calculated in the ladder approximation to the quark exchange between a scalar or axialvector diquark and a constituent quark. These functions reflecting full Lorentz covariance are given in terms of an expansion in Gegenbauer polynomials. In the rest frame of the baryon, a complete partial wave decomposition of the Bethe-Salpeter wave function is performed. The confinement of quarks and diquarks is implemented via a parametrization of the corresponding propagators. We also discuss some aspects of the momentum routing in the ladder approximation to the Bethe-Salpeter equation. Numerical results for the octet and decuplet masses with broken flavor SU(3) in the conserved isospin limit are presented. [S0556-2813(98)00810-3]

PACS number(s): 11.10.St, 12.39.Ki, 12.40.Yx, 14.20.Dh

I. INTRODUCTION

In a recent paper [1] we presented numerical results for the nucleon form factors in a fully Lorentz covariant model based on the idea that baryons may be viewed as bound states of confined constituent diquarks and quarks interacting via quark exchange. The confinement of the constituents is hereby effectively parametrized. The poles of the corresponding propagators are removed by some modifying multiplicative factors which, however, possess an essential singularity at timelike infinite momentum. The physical picture behind this baryon model is very natural: Diquarks are allowed to ''decay'' into two quarks, one of them recombines with the third quark and forms another diquark. The hope is, that for physics relevant at intermediate momentum transfers, most of the complicated structure of the baryon may be efficaciously described by assuming strong correlations in the quark-quark channel. Thus the notion of diquarks parametrizes to some extent unknown nonperturbative physics within baryons. In recent years diquarks have not only been used in nonperturbative calculations but also in the description of inelastic lepton-nucleon scattering, see Refs. [2,3] where various applications of diquarks are extensively discussed. Very recently diquark masses have been estimated from lattice measurements [4].

The main purpose of our investigations is to formulate a baryon model applicable to the intermediate energy region. This is mainly motivated with the advent of a new generation of continuous beam facilities such as CEBAF at TJNAF, MAMI, ELSA, COSY etc. which are designed to explore an intermediate region lying between the non-perturbative low-energy and the perturbative high-energy regime of QCD. These facilities explore various hadron observables to a very high precision. The different existing hadron models are to be judged by their ability to predict and to explain these observables in the near future. While there exist many models capable of describing pion properties which are strongly

dictated by chiral symmetry, the detailed structure of all other mesons are still unclear. Although quite a few baryon models, see, e.g., Refs. [5–11], have been developed in the last 40 years, a unified description of baryons within a covariant field theoretical approach, and with quarks and gluons as the fundamental degrees of freedom, is still missing. In addition to being covariant, such a description should include chiral symmetry in its spontaneously broken phase and confinement. A covariant model with the correct symmetry pattern but without confinement is the Nambu–Jona-Lasinio (NJL) model [12,13] where quarks as fundamental fermion fields interact locally, for recent reviews see Refs. [14–16]. There, baryons appear either as nontopological solitons [17–19] or as bound states of a quark and a diquark [20–26]. A hybrid formalism combining the soliton with the diquark picture has been developed in Ref. [27], where it turned out that the soliton background contributes as much to the total binding energy of the nucleon as the direct coupling between two quarks and between quark and diquark. In the Global Color Model, a nonlocal extension of the NJL model, there also exist preliminary studies of nucleons as diquark-quark bound states, see, e.g., Ref. [28] and references therein.

In this paper we extend the investigations reported in Ref. [1]. There we solved the Bethe-Salpeter equation for nucleons in the ladder approximation but restricted ourselves to scalar diquarks. Employing the solution of the Bethe-Salpeter equation, i.e., the nucleon vertex functions, we calculated various form factors such as the electromagnetic, the weak, and the pionic form factor of the nucleon. Despite the fact that this work is a promising starting point for further investigations, some results, especially for the magnetic moments, signaled that the axial-vector diquark channel is necessary for a realistic description of baryons as bound states of quarks and diquarks. Here we therefore include the axialvector diquark channel into the nucleon Bethe-Salpeter equation. We also present results for baryons with spin 3/2.

The paper is organized as follows: In the next section the covariant and confining diquark-quark model, as defined in Ref. [1], is briefly reviewed. By modifying the propagators of quarks and diquarks an effective modeling of confinement enters our model. In Sec. III the Bethe-Salpeter equations for spin-1/2 and spin-3/2 baryons, determining their masses and

_____

*E-mail: oettel@pthp3.tphys.physik.uni-tuebingen.de

†Present address: Deutsche Bank, Frankfurt, Germany.

‡E-mail: Reinhard.Alkofer@uni-tuebingen.de

wave functions, are discussed. With an appropriate three spinor basis we then construct covariant *Ansätze* for the wave functions which are suitable for the numerical solution of the homogeneous integral equations. Section IV is devoted to a discussion of the subtleties concerning the momentum routing in the Bethe-Salpeter equation, associated with the ladder approximation. The numerical method is shortly described in Sec. V, and our results for the baryon masses and wave functions are described in Sec. VI. In the last section we finally conclude and give an outlook. Some technical issues are deferred to three appendixes.

II. THE COVARIANT AND CONFINING DIQUARK-QUARK MODEL

Here we briefly recapitulate the definition of the covariant and confining diquark-quark model as given in Ref. [1]. Such a model, although without confinement, has been also considered in Refs. [29,30]. Since the solution of a rigorous relativistic three body equation, a Faddeev equation [31], is still missing in field theory we follow the path of using diquarks as effective degrees of freedom within baryons. They serve as an efficient tool to parametrize some of the unknown non-perturbative features of the baryon wave function. As stated in the Introduction such approaches have been successful in the past to describe baryons in NJL-type models [20–26]. A three-dimensional reduction of the fully covariant Bethe-Salpeter model discussed here, can be found in Ref. [32], where the author solved the bound state equations in the Salpeter approximation which ignores all retardation effects.

Having in mind the diquark-quark description arising within the hadronized NJL model [20], some basic structures are fixed: To build up a colorless baryon out of a diquark and a quark being in the fundamental representation of the color group $SU(3)_C$, diquarks necessarily live in the color antitriplet channel. Furthermore, in order to fulfill the Pauli principle, scalar diquarks couple via the antisymmetric generators of the flavor group $t_{\mathcal{A}}^a = \{\rho^{a=1..3}\}$, axial-vector diquarks via the symmetric generators $t_{\mathcal{S}}^a = \{\rho^{a=4..9}\}$, respectively [20]. Our conventions for these flavor matrices ρ^a are given in Appendix A. In the following, however, we deviate from the NJL model as described in Ref. [16]. Quarks and diquarks are treated as elementary but confined particles, see below, whose interaction, quark exchange, gives rise to quark-diquark correlations strong enough to bind these fields to a baryon.

This can be formalized with the Lagrangian

$$\mathcal{L} = \bar{q}_A(x)(i\gamma^\mu \partial_\mu - \mathbf{m}_q)f(-\partial^2/\mathbf{m}_q^2)q_A(x)$$

$$+ \Delta_A^\dagger(x)(-\partial_\mu \partial^\mu - \mathbf{m}_{0^+}^2)f(-\partial^2/\mathbf{m}_{0^+}^2)\Delta_A(x)$$

$$- \frac{1}{4}F_{\mu\nu}^\dagger(x)f(-\partial^2/\mathbf{m}_{1^+}^2)F^{\mu\nu}(x)$$

$$+ \frac{1}{2}\mathbf{m}_{1^+}^2\Delta_{Aa\mu}^\dagger(x)f(-\partial^2/\mathbf{m}_{1^+}^2)\Delta_{Aa}^\mu(x)$$

$$+ \epsilon^{ABC}(g_s q_C^T(x)Ci\gamma^5 t_{\mathcal{A}}^a q_B(x)\Delta_{aA}^*(x)$$

$$+ g_s^* \Delta_{aA}(x)\bar{q}_B(x)i\gamma^5 Ct_{\mathcal{A}}^{\dagger a}\bar{q}_C^{-T}(x))$$

$$+ \epsilon^{ABC}(g_a q_C^T(x)Ci\gamma^\mu t_{\mathcal{S}}^a q_B(x)\Delta_{Aa\mu}^*(x)$$

$$- g_a^* \Delta_{Aa\mu}(x)\bar{q}_B(x)t_{\mathcal{S}}^{\dagger a}i\gamma^\mu C\bar{q}_C^{-T}(x)). \tag{2.1}$$

The quark field is denoted by $q(x)$, the scalar diquark field by $\Delta(x)$ and the axial-vector diquark field by $\Delta^\mu(x)$. Their masses are given by the matrices in flavor space $\mathbf{m}_q$, $\mathbf{m}_{0^+}$ and $\mathbf{m}_{1^+}$, respectively. For unbroken flavor symmetry they reduce to $\mathbf{m}_q = \mathrm{diag}_3(m_q)$, $\mathbf{m}_{0^+} = \mathrm{diag}_3(m_{0^+})$, and $\mathbf{m}_{1^+} = \mathrm{diag}_6(m_{1^+})$. In Eq. (2.1), capital subscripts denote color quantum numbers. In the kinetic part of the 1^+ diquark the non-Abelian field strength tensor $F^{\mu\nu} = \partial^\mu \Delta^\nu - \partial^\nu \Delta^\mu + [\Delta^\mu, \Delta^\nu]$ appears $(\Delta_\mu = \Delta_{a\mu}t_{\mathcal{S}}^a)$. The associated self-interactions, however, will not be taken into account. The coupling strengths, of Yukawa type, between two quarks and the scalar or axial-vector diquarks are given by g_s or g_a, respectively. In order to take an extended diquark into account, the pointlike couplings will be supplemented with momentum dependent factors to be defined later.

An essential ingredient entering our model is the effective parametrization of confinement. This is realized by modifying the kinetic terms of the constituents in the Lagrangian (2.1). Going to Euclidean[1] momentum space and using

$$f^{-1}(x) = 1 - e^{-d(1+x)}. \tag{2.2}$$

the model quark and diquark propagators, being diagonal in color and flavor space, are given by

$$S(p) = \frac{i\not{p} - m_q}{p^2 + m_q^2}(1 - e^{-d(p^2 + m_q^2)/m_q^2}), \tag{2.3}$$

$$D(p) = -\frac{1}{p^2 + m_{0^+}^2}(1 - e^{-d(p^2 + m_{0^+}^2)/m_{0^+}^2}), \tag{2.4}$$

$$D^{\mu\nu}(p) = -\frac{(\delta^{\mu\nu} + p^\mu p^\nu/m_{1^+}^2)}{p^2 + m_{1^+}^2}(1 - e^{-d(p^2 + m_{1^+}^2)/m_{1^+}^2}). \tag{2.5}$$

Due to the numerators, the mass poles of the propagators are effectively screened.[2] The strength of the screening is described by the parameter d. Whereas the analytic behavior of the quark propagator (2.3) is similar to the ones obtained from Dyson-Schwinger studies of QCD (details about this approach can be found in Ref. [33]), the justification for using confined diquarks is somewhat more involved. As stated above, diquarks are not color singlets and should therefore be confined by the fundamental interaction of QCD. Nevertheless most diquark models [34–36] which describe them as bound states of two quarks predict diquarks to be observable particles. Recent studies, however, which investigated the system of the quark Dyson-Schwinger equation and the diquark Bethe-Salpeter equation beyond the usu-

---

[1] We use an Euclidean space formulation with $\{\gamma_\mu, \gamma_\nu\} = 2\delta_{\mu\nu}$, $\gamma_\mu^\dagger = \gamma_\mu$ and $pq = \Sigma_{\mu=1}^4 p_\mu q_\mu$.

[2] With $f \equiv 1$ we refer to the propagators as tree level propagators.

ally employed rainbow-ladder approximation, were able to explain why diquarks do not appear in the observable particle spectrum. This mechanism works in the Munczek-Nemirovsky model [37], as has been shown in Ref. [38], as well as in an extended NJL model [39]. Since both models assume a simplified but quite different quark-quark interaction, one may conjecture that the same also holds true implementing a realistic interaction. For these reasons we use the notion of confined diquarks. In our approach we therefore use the propagators defined in Eqs. (2.4) and (2.5) which do not allow observable diquarks. In the following it will be seen that working with confined quarks and diquarks leads to the absence of an unphysical quark-diquark threshold for baryons.

Additionally we introduce the diagonal approximation to the axial-vector diquark propagator by omitting the $p^\mu p^\nu/m_{1+}^2$ term,

$$D^{\mu\nu}(p) = -\frac{\delta^{\mu\nu}}{p^2+m_{1+}^2}f^{-1}\left(\frac{p^2}{m_{1+}^2}\right). \qquad (2.6)$$

It is well-known that the full Proca propagator may cause spurious ultraviolet problems. These vanish in the special, unitary gauge and have no physical consequences. As such a treatment is, however, beyond the scope of our purely phenomenological investigation we have chosen to avoid this problem by using a diagonal approximation to the propagator. Its validity is examined more closely in Appendix B.

III. BETHE-SALPETER EQUATION FOR OCTET AND DECUPLET BARYONS IN THE FLAVOR-SYMMETRIC CASE

Using the Lagrangian given in Eq. (2.1) we obtain the ladder Bethe-Salpeter equation for octet and decuplet baryons

$$\begin{pmatrix} \Psi_8(p;P) \\ \Psi_8^\nu(p;P) \end{pmatrix}$$

$$= -|g_s|^2 \begin{pmatrix} D(p_b) & 0 \\ 0 & D^{\nu\mu}(p_b) \end{pmatrix} S(p_a) \int \frac{d^4p'}{(2\pi)^4}$$

$$\times \begin{pmatrix} \gamma_5\tilde{S}(-q)\gamma_5 & -\sqrt{3}\frac{g_a}{g_s}\gamma^{\mu'}\tilde{S}(-q)\gamma_5 \\ -\sqrt{3}\frac{g_a^*}{g_s^*}\gamma_5\tilde{S}(-q)\gamma^\mu & -\frac{|g_a|^2}{|g_s|^2}\gamma^{\mu'}\tilde{S}(-q)\gamma^\mu \end{pmatrix}$$

$$\times \begin{pmatrix} \Psi_8(p';P) \\ \Psi_8^{\mu'}(p';P) \end{pmatrix}, \qquad (3.1)$$

$$\Psi_{10}^{\nu\rho}(p;P) = -2|g_a|^2 S(p_a)D^{\nu\mu}(p_b)$$

$$\times \int \frac{d^4p'}{(2\pi)^4}\gamma^\lambda\tilde{S}(-q)\gamma^\mu\Psi_{10}^{\lambda\rho}(p';P). \qquad (3.2)$$

In this formulation, the Bethe-Salpeter equation involves the matrix-valued Bethe-Salpeter wave functions of octet baryons $\Psi_8(p;P)$ and $\Psi_8^\nu(p;P)$ and decuplet baryons $\Psi_{10}^{\lambda\nu}(p;P)$, respectively, which are projected on positive parity and spin 1/2 or spin 3/2 (see the following subsection for their construction). Their flavor part is given by pure octet and decuplet states in $SU(3)_{\text{flavor}}$. They depend on the total momentum P of the bound state and on the relative momentum p' or p between the two constituents. Mathematically, the Bethe-Salpeter equations are equivalent to coupled homogeneous integral equations. The numerical method for its solution is presented in Sec. V, see also [40].

Although the Lagrangian (2.1) describes a renormalizable diquark-quark theory, at least at one-loop level, the Bethe-Salpeter equations in ladder approximation are formally divergent in the ultraviolet. The divergence, of course, should then be cured by the wave functions. However, to crudely take into account the extended nature of diquarks we work, as in Ref. [30,1], with a finite interaction in momentum space and modify the propagator of the exchanged quark according to

$$S(q) \to \tilde{S}(q) = S(q)\left(\frac{\Lambda^2}{q^2+\Lambda^2}\right). \qquad (3.3)$$

This corresponds to a monopole-type form factor. As a consequence, this also removes all formal ultraviolet divergencies. Note that we have absorbed the charge conjugation matrix C appearing in the Lagrangian (2.1) using the identity $C^{-1}\tilde{S}^T(q)C = \tilde{S}(-q)$.

Before actually solving the integral equations it is appropriate to find a suitable basis for the wave functions appearing in Eqs. (3.1) and (3.2).

A. Relativistic three quark states and their wave functions

When constructing a baryon out of three quarks, its wave function is formally described by a spinor of rank three, $\psi_{\alpha\beta\gamma}$ ($\alpha,\beta,\gamma=1\ldots4$). For octet baryons, a convenient basis for this multi-spinor can be found by expanding the direct product of the spinors describing quarks of flavor b and c with spinor indices β and γ into the complete set of Dirac matrices and taking the direct product with a spinor basis of quark a [41]:

$$\psi_{\alpha\beta\gamma}^8 = (\Gamma u)_\alpha(\phi C\gamma_5)_{\beta\gamma}. \qquad (3.4)$$

C denotes charge conjugation and

$$u = \left\{\begin{pmatrix} \chi^+ \\ 0 \end{pmatrix}, \begin{pmatrix} \chi^- \\ 0 \end{pmatrix}\right\}$$

is a basis of positive energy Dirac spinors in the rest frame describing fermions with spin up ($+$) and spin down ($-$). In this representation Γ and ϕ are Dirac matrices to be expanded in the complete set $\{\mathbf{1},\gamma_5,\gamma^\mu,\gamma_5\gamma^\mu,\sigma^{\mu\nu}\}$.

Under a Lorentz transformation $S(\Lambda)$, this wave function transforms according to

$$\psi_{\alpha\beta\gamma}^8 = (S\Gamma(\Lambda^{-1}P,\Lambda^{-1}p)S^{-1})_{\alpha\alpha'}(Su)_{\alpha'}(S\phi S^{-1}C\gamma_5)_{\beta\gamma}. \qquad (3.5)$$

TABLE I. The Lorentz covariants leading to baryons with positive parity. They are grouped according to their diquark content.

	Scalar diquark $(C\gamma_5)_{\beta\gamma}$	Axial-vector diquark $(\gamma_\mu\gamma_5 C\gamma_5)_{\beta\gamma}$
Octet	$(\Gamma_i^S u)_\alpha$	$(\Gamma_i^{A\mu} u)_\alpha$
Decuplet		$(\Gamma_i^S u^\mu)_\alpha$
		$(\gamma_5 \Gamma_i^{A\mu}[p_T^\nu u_\nu])_\alpha$
$\Gamma_i^S \in$	$\{\mathbf{1}, \not{P}, \not{p}, P_\mu\sigma^{\mu\nu}p_\nu\}$	
$\Gamma_i^{A\mu} \in$	$\{P^\mu\gamma_5, p^\mu\gamma_5, \gamma^\mu\gamma_5, P^\mu\gamma_5\not{P}, P^\mu\gamma_5\not{p},$	
	$p^\mu\gamma_5\not{P}, p^\mu\gamma_5\not{p}, P_\nu\gamma_5\sigma^{\nu\mu}, p_\nu\gamma_5\sigma^{\nu\mu},$	
	$P^\mu\gamma_5 P_\nu\sigma^{\nu\rho}p_\rho, p^\mu\gamma_5 P_\nu\sigma^{\nu\rho}p_\rho, \gamma^\mu\gamma_5 P_\nu\sigma^{\nu\rho}p_\rho\}$	

The parity transformation is given by

$$\psi^8_{\alpha\beta\gamma} = \pi(\gamma^4\Gamma(\widetilde{\gamma}^\mu, \widetilde{P}, \widetilde{p})u)_\alpha(\gamma^4\phi(\widetilde{\gamma}^\mu, \widetilde{P}, \widetilde{p})\gamma^4 C\gamma_5)_{\beta\gamma}, \tag{3.6}$$

where π is the intrinsic parity of the baryon and $\widetilde{P} = (-\mathbf{P}, P^4)$, $\widetilde{p} = (-\mathbf{p}, p^4)$, $\widetilde{\gamma}^\mu = (-\boldsymbol{\gamma}, \gamma^4)$.

To ensure total spin 1/2 of the wave function, the free Lorentz indices in (3.4) are to be contracted with the independent momenta involved and each covariant will be multiplied by a scalar function.

In the diquark-quark model, only the two choices for $\phi = \{\mathbf{1}, \gamma^\mu\gamma_5\}$ are taken into account which describe the scalar and axial-vector diquark. The covariants which lead to positive parity of spin-1/2 octet states, $(\Gamma u)_\alpha$, can be grouped according to scalar and axial-vector diquark states with the spinor indices β and γ, see Table I, second row. As described above, the free Lorentz indices in these covariants are contracted with the momenta P and p and are then to be multiplied with scalar functions. No further symmetrization of the wave function is necessary as this will be provided by the quark exchange.

Using this classification scheme, the octet wave function can be denoted by

$$\psi^8_{\alpha\beta\gamma} = \sum_{i=1}^4 (Z_i^S\Gamma_i^S u)_\alpha(C\gamma_5)_{\beta\gamma} + \sum_{i=5}^{16} (Z_i^A\Gamma_i^{A\mu} u)_\alpha(\gamma_\mu C)_{\beta\gamma}. \tag{3.7}$$

Each of the four covariants Γ_S^i which describe the scalar diquark part in the octet baryon wave function is multiplied by a scalar function Z_i^S and likewise there are twelve scalar functions Z_i^A multiplying the axial-vector diquark covariants $\Gamma_i^{A\mu}$.

A further reduction of this *Ansatz* by a projection to positive energies is very convenient. From the expression (3.7) for the octet wave function we consider only the part with spinor index α, multiply it with the adjoint spinor $\bar{u}(P,s)$ and sum over the spins. This leads to a wave function which is, by construction, an eigenfunction of the positive-energy

projector[3] $\Lambda^+ = (1 + \hat{\not{P}})$. Thus we are led to the following relations between the wave functions of Eq. (3.7) and the corresponding functions in the Bethe-Salpeter equation (3.1):

$$\begin{pmatrix} Z_i^S\Gamma_i^S \\ Z_i^A\Gamma_i^{A\mu} \end{pmatrix}\Lambda^+ = \begin{pmatrix} S_i\mathcal{S}_i \\ A_i\mathcal{A}_i^\mu \end{pmatrix} = \begin{pmatrix} S_i\mathcal{S}_i \\ A_i\mathcal{A}_i^\mu \end{pmatrix}\Lambda^+ = \begin{pmatrix} \Psi_8(p;P) \\ \Psi_8^\mu(p;P) \end{pmatrix}. \tag{3.8}$$

The independent covariants $\mathcal{S}_i$ and $\mathcal{A}_i^\mu$ are required to be eigenfunctions of Λ^+ which reduces the number of independent scalar functions from sixteen to eight which are now denoted by S_i, $(i=1,2)$ and A_i, $(i=1\dots6)$. A convenient representation of these covariants suitable for our numerical procedure and for further applications is given by

$$\mathcal{S}_i = \begin{cases} \mathcal{S}_1 = \Lambda^+, \\ \\ \mathcal{S}_2 = -\dfrac{i}{p}\not{p}_T\Lambda^+, \end{cases} \tag{3.9}$$

$$\mathcal{A}_i^\mu = \begin{cases} \mathcal{A}_1^\mu = -\dfrac{i}{p}\hat{P}^\mu\gamma_5\not{p}_T\Lambda^+, \\ \mathcal{A}_2^\mu = \hat{P}^\mu\gamma_5\Lambda^+, \\ \mathcal{A}_3^\mu = \hat{p}_T^\mu\gamma_5\hat{\not{p}}_T\Lambda^+, \\ \mathcal{A}_4^\mu = \dfrac{i}{p}p_T^\mu\gamma_5\Lambda^+, \\ \mathcal{A}_5^\mu = \gamma_5\gamma_T^\mu\Lambda^+ - \mathcal{A}_3^\mu, \\ \mathcal{A}_6^\mu = \dfrac{i}{p}\gamma_5\gamma_T^\mu\not{p}_T\Lambda^+ - \mathcal{A}_4^\mu, \end{cases} \tag{3.10}$$

where $\gamma_T^\mu = \gamma^\mu - \hat{P}^\mu\hat{\not{P}}$. Note that the indices have been chosen such that matrices with odd indices $i=\{1,3,5\}$ are eigenfunctions to $\not{P} - iM$ whereas the ones with even indices $i=\{2,4,6\}$ are eigenfunctions to $\not{P} + iM$, with eigenvalue 0 in both cases.

---

[3]We denote normalized four vectors with a hat, e.g., $\hat{P}\cdot\hat{P} = 1$. In the Euclidean rest frame $P = (\mathbf{0}, iM)$ this explicitly reads $\hat{P} = P/iM$. Note that all relative momenta (p, p') are real in Euclidean space as they are only needed for spacelike values.

In the rest frame of the bound state, $P=(\mathbf{0},iM)$, the *Ansatz* for the matrix valued nucleon wave function which we used for further numerical processing reads

$$
\begin{pmatrix} \Psi_8(p;P) \\ \Psi_8^4(p;P) \\ \Psi_8(p;P) \end{pmatrix} = \begin{pmatrix} \begin{pmatrix} \mathbf{1}S_1 & 0 \\ \frac{1}{p}(\boldsymbol{\sigma}\mathbf{p})S_2 & 0 \end{pmatrix} \\ \begin{pmatrix} \frac{1}{p}(\boldsymbol{\sigma}\mathbf{p})A_1 & 0 \\ \mathbf{1}A_2 & 0 \end{pmatrix} \\ \begin{pmatrix} i\hat{\mathbf{p}}(\boldsymbol{\sigma}\hat{\mathbf{p}})A_3+(\boldsymbol{\sigma}\times\hat{\mathbf{p}})(\boldsymbol{\sigma}\hat{\mathbf{p}})A_5 & 0 \\ \frac{i}{p}\mathbf{p}A_4+\frac{1}{p}(\boldsymbol{\sigma}\times\mathbf{p})A_6 & 0 \end{pmatrix} \end{pmatrix}.
$$

$$(3.11)$$

The scalar quantities S_i and A_i depend on $p=\sqrt{p_\mu p_\mu}$ and $z=\cos\psi=\hat{P}\cdot\hat{p}$ for each value of the bound state mass. As expected from the properties of $\mathcal{S}_i$ and $\mathcal{A}_i^\mu$ [see Eqs. (3.9) and (3.10)], upper components have odd indices, lower components have even indices.

The strategy shown above for the octet baryon can also be applied to decuplet baryons which have spin 3/2. Projection of the trispinor wave function $\psi_{\alpha\beta\gamma}$ onto total spin 3/2 may be achieved by expanding the piece associated with quark a in terms of Rarita-Schwinger spinors u_μ:

$$\psi_{\alpha\beta\gamma}^{10}=(\Gamma u_\mu)_\alpha(\phi C)_{\beta\gamma},\qquad(3.12)$$

Γ is chosen such that all Lorentz indices are contracted with the momenta P and p. Note that the Rarita-Schwinger constraints demand $u_\mu\gamma^\mu=u_\mu P^\mu=0$ and that in the diquark-quark model the diquark part of decuplet states is made of axial-vector diquarks only, $\phi=C\gamma^\nu$.

The covariants Γ which are left for decuplet states after applying the above restrictions and the positive parity constraint can be found in Table I, third row. The covariants for octet and decuplet states are closely related. Due to the Rarita-Schwinger constraints the Lorentz index of u_μ must be contracted either with the Lorentz index of the axial-vector diquark ($\gamma^\mu C$) or with the transversal relative momentum $p_T^\mu=p^\mu-\hat{P}^\mu(p\cdot\hat{P})$. For the first choice, we have the same four covariants as for the octet state with scalar diquark correlations. For the second choice, we obtain the

twelve covariants as for the octet state with axial-vector diquark correlations, however, multiplied by γ_5 to ensure positive parity. The decuplet wave functions read now

$$
\psi_{\alpha\beta\gamma}^{10}=(\Upsilon_{10}^{\mu\nu}u^\nu)_\alpha(\gamma_\mu C)_{\beta\gamma}
$$

$$
=\sum_{i=1}^{4}(Z_i^D\Gamma_i^S\delta^{\mu\nu}u^\nu)_\alpha(\gamma_\mu C)_{\beta\gamma}
$$

$$
+\sum_{i=5}^{16}(Z_i^D\gamma_5\Gamma_i^{A\mu}\hat{p}_T^\nu u^\nu)_\alpha(\gamma_\mu C)_{\beta\gamma},\quad(3.13)
$$

where the Z_i^D denote the sixteen scalar functions for the decuplet state.

Taking from eq. (3.13) only the part with spinor index α and projecting it to positive energies leads to

$$
\sum_{s=-3/2}^{+3/2}\Upsilon_{10}^{\mu\nu}(p;P)u^\nu(P,s)\bar{u}^\lambda(P,s)
$$

$$
=\Upsilon_{10}^{\mu\nu}(p;P)\mathbf{P}^{\nu\lambda}=\Psi_{10}^{\mu\nu}(p;P)=\Psi_{10}^{\mu\lambda}(p;P)\mathbf{P}^{\lambda\nu}.
$$

$$(3.14)$$

Therefore the projected wave function (which besides being a 4×4 matrix has tensor character) is determined by the condition

$$\Psi_{10}^{\mu\nu}(p;P)=\Psi_{10}^{\mu\lambda}(p;P)\mathbf{P}^{\lambda\nu},\qquad(3.15)$$

which requires $\Psi_{10}^{\mu\nu}$ to be an eigenfunction of the Rarita-Schwinger projector. Here, the explicit expression of the Euclidean Rarita-Schwinger projector is given by

$$
\mathbf{P}^{\mu\nu}:=\Lambda^+\left(-\delta^{\mu\nu}+\frac{1}{3}\gamma^\mu\gamma^\nu-\frac{2}{3}\frac{P^\mu P^\nu}{M^2}+\frac{i}{3}\frac{P^\mu\gamma^\nu-P^\nu\gamma^\mu}{M}\right)
$$

$$=:\Lambda^+\Lambda^{\mu\nu}.\qquad(3.16)$$

The most general form which fulfills condition (3.15) is

$$\Psi_{10}^{\mu\nu}(p;P)=D_i\mathcal{S}_i\Lambda^+\Lambda^{\mu\nu}+iE_i\gamma_5\mathcal{A}_i^\mu\Lambda^+\hat{p}_T^\lambda\Lambda^{\lambda\nu}$$

$$(3.17)$$

which requires the covariants again to be eigenfunctions of Λ^+, as a consequence we may use the same choice for the $\mathcal{A}_i^\mu$ and $\mathcal{S}_i$ as in the octet case and are left with eight independent scalar functions.

In the rest frame of the bound state, the decuplet wave functions are then denoted by

$$
\Psi_{10}^{ij}(p;P)=\begin{pmatrix}\left(\delta^{ij}-\frac{1}{3}\sigma^i\sigma^j\right)D_1 & 0 \\ \frac{1}{p}(\boldsymbol{\sigma}\mathbf{p})\left(\delta^{ij}-\frac{1}{3}\sigma^i\sigma^j\right)D_2 & 0\end{pmatrix}+\begin{pmatrix}[-\hat{p}^iE_4+i(\boldsymbol{\sigma}\times\hat{\mathbf{p}})^iE_6]\left[\hat{p}^j-\frac{1}{3}(\boldsymbol{\sigma}\hat{\mathbf{p}})\sigma^j\right] & 0 \\ \frac{1}{p}[-\hat{p}^iE_3+i(\boldsymbol{\sigma}\times\hat{\mathbf{p}})^iE_5](\boldsymbol{\sigma}\mathbf{p})\left[\hat{p}^j-\frac{1}{3}(\boldsymbol{\sigma}\hat{\mathbf{p}})\sigma^j\right] & 0\end{pmatrix}
$$

$$(3.18)$$

$$
\Psi_{10}^{4j}(p;P)=\begin{pmatrix}\frac{i}{p}\left[p^j-\frac{1}{3}(\boldsymbol{\sigma}\mathbf{p})\sigma^j\right]E_2 & 0 \\ i(\boldsymbol{\sigma}\hat{\mathbf{p}})\left[\hat{p}^j-\frac{1}{3}(\boldsymbol{\sigma}\hat{\mathbf{p}})\sigma^j\right]E_1 & 0\end{pmatrix}
$$

and all other components of $\Psi_{10}^{\mu\nu}(p;P)$ vanish. The appearance of γ_5 in Eq. (3.17) has interchanged upper and lower components as compared to the octet case.

Instead of working with the Bethe-Salpeter wave functions one may alternatively use the Bethe-Salpeter vertex functions obtained by amputating the external quark and diquark propagators from the wave function

$$\Phi_8(p;P)=S^{-1}(p_a)D^{-1}(p_b)\Psi_8(p;P), \qquad (3.19)$$

$$\Phi_8^\mu(p;P)=S^{-1}(p_a)(D^{-1})^{\mu\nu}(p_b)\Psi_8^\nu(p;P), \quad (3.20)$$

$$\Phi_{10}^{\mu\rho}(p;P)=S^{-1}(p_a)(D^{-1})^{\mu\nu}(p_b)\Psi_{10}^{\nu\rho}(p;P). \quad (3.21)$$

Substituting the wave functions by the vertex functions in the Bethe-Salpeter equations (3.1) and (3.2) leads to a reformulation of the bound state equations which is sometimes more convenient. For example in Refs. [30,1] the equations containing only scalar diquarks have been solved in a form which includes the vertex function explicitly.

B. Orbital angular momentum and spin of the Bethe-Salpeter wave functions in the rest frame of the bound state

Whereas the choice of the covariants in Eqs. (3.9) and (3.10) which build the octet and decuplet wave functions is well suited for numerical computation and further covariant calculations, their physical interpretation is not obvious. In general, covariant wave functions possess only the mass of the bound state M and its total angular momentum J as good quantum numbers. In the rest frame of the bound state, however, the wave functions can be written as a sum of trispinors each possessing definite orbital angular momentum and spin, thus allowing a direct interpretation of the different components. These trispinors are linear combinations of the covariants $\mathcal{S}_i$ and $\mathcal{A}_i$ which have been constructed in the previous subsection, multiplied by the respective Dirac matrices $(\gamma_5 C)_{\beta\gamma}$ and $(\gamma^\mu C)_{\beta\gamma}$ denoting the diquark content, respectively.

In the rest frame the Pauli-Lubanski operator for a trispinor is given by

$$W^i=\frac{1}{2}\epsilon_{ijk}\mathcal{L}^{jk}, \qquad (3.22)$$

whose square characterizes the total angular momentum

$$W^iW^i\psi_{\alpha\beta\gamma}=J(J+1)\psi_{\alpha\beta\gamma}. \qquad (3.23)$$

Here, $\psi_{\alpha\beta\gamma}$ is the trispinor wave function with positive parity and positive energy. The tensor $\mathcal{L}^{jk}$ is the sum of an orbital part L^{jk} and a spin part S^{jk} which read

$$L^{jk}=\sum_{a=1}^{3}(-i)\left(p_a^j\frac{\partial}{\partial p_a^k}-p_a^k\frac{\partial}{\partial p_a^j}\right), \qquad (3.24)$$

$$2(S^{jk})_{\alpha\alpha',\beta\beta',\gamma\gamma'}=(\sigma^{jk})_{\alpha\alpha'}\otimes\delta_{\beta\beta'}\otimes\delta_{\gamma\gamma'}+\delta_{\alpha\alpha'}\otimes(\sigma^{jk})_{\beta\beta'}$$
$$\otimes\delta_{\gamma\gamma'}+\delta_{\alpha\alpha'}\otimes\delta_{\beta\beta'}\otimes(\sigma^{jk})_{\gamma\gamma'}, \quad (3.25)$$

such that $\mathcal{L}^{jk}=L^{jk}+\frac{1}{2}S^{jk}$. Obviously, L^{jk} is proportional to the unit matrix in Dirac space. The definition of $\sigma^{\mu\nu}$:

$=-(i/2)[\gamma^\mu,\gamma^\nu]$ differs by a minus sign from its Minkowski counterpart. The tensors L and S are written as a sum over the respective tensors for each of the three constituent quarks which are labeled $a=1,\ldots,3$ and with respective Dirac indices $\alpha\alpha',\beta\beta',\gamma\gamma'$.

With the definition of the spin matrix $\Sigma^i=\frac{1}{2}\epsilon_{ijk}\sigma^{jk}$ the Pauli-Lubanski operator reads

$$(W^i)_{\alpha\alpha',\beta\beta',\gamma\gamma'}=L^i\delta_{\alpha\alpha'}\otimes\delta_{\beta\beta'}\otimes\delta_{\gamma\gamma'}+(S^i)_{\alpha\alpha',\beta\beta',\gamma\gamma'}, \qquad (3.26)$$

$$L^i=(-i)\epsilon_{ijk}p^j\frac{\partial}{\partial p^k}, \qquad (3.27)$$

$$(S^i)_{\alpha\alpha',\beta\beta',\gamma\gamma'}=\frac{1}{2}[(\Sigma^i)_{\alpha\alpha'}\otimes\delta_{\beta\beta'}\otimes\delta_{\gamma\gamma'}+\delta_{\alpha\alpha'}\otimes(\Sigma^i)_{\beta\beta'}$$
$$\otimes\delta_{\gamma\gamma'}+\delta_{\alpha\alpha'}\otimes\delta_{\beta\beta'}\otimes(\Sigma^i)_{\gamma\gamma'}], \qquad (3.28)$$

where we have already introduced the relative momentum p between quark and diquark via a canonical transformation

$$P=p^1+p^2+p^3, \quad p=\eta(p^1+p^2)-(1-\eta)p^3,$$

$$p'=\frac{1}{2}(p^1-p^2). \qquad (3.29)$$

Assuming a pointlike diquark, the relative momentum between quark 1 and 2, p', vanishes and the only contribution to the orbital angular momentum stems from p. $\mathbf{W}^2$ now takes the form

$$\mathbf{W}^2=\mathbf{L}^2+2\mathbf{L}\cdot\mathbf{S}+\mathbf{S}^2, \qquad (3.30)$$

$$\mathbf{L}^2=\left(2p^i\frac{\partial}{\partial p^i}-\boldsymbol{p}^2\Delta_p+p^ip^j\frac{\partial}{\partial p^i}\frac{\partial}{\partial p^j}\right), \qquad (3.31)$$

$$2(\mathbf{L}\cdot\mathbf{S})_{\alpha\alpha',\beta\beta',\gamma\gamma'}=-\epsilon_{ijk}p^j\frac{\partial}{\partial p^k}\{(\Sigma^i)_{\alpha\alpha'}\otimes\delta_{\beta\beta'}\otimes\delta_{\gamma\gamma'}$$
$$+\delta_{\alpha\alpha'}\otimes[(\Sigma^i)_{\beta\beta'}\otimes\delta_{\gamma\gamma'}$$
$$+\delta_{\beta\beta'}\otimes(\Sigma^i)_{\gamma\gamma'}]\}, \qquad (3.32)$$

$$(\mathbf{S}^2)_{\alpha\alpha',\beta\beta',\gamma\gamma'}=\frac{1}{4}\{9\,\delta_{\alpha\alpha'}\otimes\delta_{\beta\beta'}\otimes\delta_{\gamma\gamma'}$$
$$+2\,\delta_{\alpha\alpha'}\otimes[(\Sigma^i)_{\beta\beta'}\otimes\delta_{\gamma\gamma'}$$
$$+\delta_{\beta\beta'}\otimes(\Sigma^i)_{\gamma\gamma'}]$$
$$+2\delta_{\alpha\alpha'}\otimes(\Sigma^i)_{\beta\beta'}\otimes(\Sigma^i)_{\gamma\gamma'}\}. \qquad (3.33)$$

When applying $\mathbf{W}^2$ to the wave functions we first note that a scalar function does not contribute to the angular momentum, e.g.,

$$\mathbf{L}^2S_1(p^2,iMp_4)=2\mathbf{L}\cdot\mathbf{S}\,S_1(p^2,iMp_4)=0. \qquad (3.34)$$

TABLE II. Classification of the components of the octet wave function in terms of eigenstates of $\mathbf{L}^2$ and $\mathbf{S}^2$ in the rest frame of the bound state.

$\psi^8_{\alpha\beta\gamma}$ in the rest frame	eigenvalue $l(l+1)$ of $\mathbf{L}^2$	eigenvalue $s(s+1)$ of $\mathbf{S}^2$
$\mathcal{S}_1 u(\gamma_5 C) = \begin{pmatrix} \chi \\ 0 \end{pmatrix}(\gamma_5 C)$	0	$\frac{3}{4}$
$\mathcal{S}_2 u(\gamma_5 C) = \begin{pmatrix} 0 \\ \frac{1}{p}(\boldsymbol{\sigma p})\chi \end{pmatrix}(\gamma_5 C)$	2	$\frac{3}{4}$
$\mathcal{A}_1^\mu u(\gamma^\mu C) = \hat{P}^0 \begin{pmatrix} \frac{1}{p}(\boldsymbol{\sigma p})\chi \\ 0 \end{pmatrix}(\gamma^4 C)$	2	$\frac{3}{4}$
$\mathcal{A}_2^\mu u(\gamma^\mu C) = \hat{P}^0 \begin{pmatrix} 0 \\ \chi \end{pmatrix}(\gamma^4 C)$	0	$\frac{3}{4}$
$\mathcal{B}_1^\mu u(\gamma^\mu C) = \begin{pmatrix} i\sigma^i\chi \\ 0 \end{pmatrix}(\gamma^i C)$	0	$\frac{3}{4}$
$\mathcal{B}_2^\mu u(\gamma^\mu C) = \begin{pmatrix} 0 \\ \frac{i}{p}\sigma^i(\boldsymbol{\sigma p})\chi \end{pmatrix}\gamma^i C$	2	$\frac{3}{4}$
$\mathcal{C}_1^\mu u(\gamma^\mu C) = \begin{pmatrix} i(\hat{p}^i(\boldsymbol{\sigma\hat{p}}) - \frac{1}{3}\sigma^i)\chi \\ 0 \end{pmatrix}(\gamma^i C)$	6	$\frac{15}{4}$
$\mathcal{C}_2^\mu u(\gamma^\mu C) = \begin{pmatrix} 0 \\ \frac{i}{p}(p^i - \frac{1}{3}\sigma^i(\boldsymbol{\sigma p})) \end{pmatrix}(\gamma^i C)$	2	$\frac{15}{4}$

In Table II we express all terms of the octet wave function in terms of eigenstates of $\mathbf{L}^2$ and $\mathbf{S}^2$. To this end we define the following linear combinations of matrices:

$$\mathcal{B}_1^\mu = \mathcal{A}_5^\mu + \mathcal{A}_3^\mu,$$

$$\mathcal{B}_2^\mu = \mathcal{A}_6^\mu + \mathcal{A}_4^\mu,$$

$$\mathcal{C}_1^\mu = -\frac{1}{3}\mathcal{A}_5^\mu + \frac{2}{3}\mathcal{A}_3^\mu,$$

$$\mathcal{C}_2^\mu = -\frac{1}{3}\mathcal{A}_6^\mu + \frac{2}{3}\mathcal{A}_4^\mu. \qquad (3.35)$$

The eigenvalue of $\mathbf{W}^2$ is $\frac{3}{4}$ for all terms, of course. In the table, $\chi = \{\chi^+, \chi^-\}$ denotes an arbitrary Pauli two-component spinor which is the positive energy basis for quark a with Dirac index α. To derive this, the following relations between Dirac matrices have proven to be useful:

$$\Sigma^j(\gamma_5 C) + (\gamma_5 C)(\Sigma^j)^T = 0 \qquad (3.36)$$

$$\Sigma^j \left(\begin{pmatrix} (\gamma^4 C) \\ (\gamma^i C) \end{pmatrix} \right) + \left(\begin{pmatrix} (\gamma^4 C) \\ (\gamma^i C) \end{pmatrix} \right)(\Sigma^j)^T = \begin{pmatrix} 0 \\ 2i\epsilon_{mji}(\gamma^m C) \end{pmatrix}, \qquad (3.37)$$

$$\Sigma^j(\gamma_5 C)(\Sigma^j)^T = -3(\gamma_5 C), \qquad (3.38)$$

$$\Sigma^j \begin{pmatrix} (\gamma^4 C) \\ (\gamma^i C) \end{pmatrix}(\Sigma^j)^T = \begin{pmatrix} -3(\gamma^4 C) \\ (\gamma^i C) \end{pmatrix}. \qquad (3.39)$$

Three covariants can be regarded as ''s-wave'' components, $\mathcal{S}_1$, $\mathcal{A}_2$, and $\mathcal{B}_1$, and we expect the corresponding scalar functions to dominate the wave function decomposition. The other ''p-, d-wave'' components represent all remaining possibilities of combining orbital angular momentum between quark and diquark and the joint spin of axial-vector diquark and quark to total spin 1/2. In this sense the description is closed.

The individual terms of the decuplet wave function can be classified accordingly with the help of the linear combinations

$$\mathcal{D}_1 = \mathcal{S}_1, \qquad (3.40)$$

$$\mathcal{D}_2^{\mu\nu} = \mathcal{S}_2\delta^{\mu\nu} + \frac{2i}{3}\gamma_5(\mathcal{A}_5^\mu + \mathcal{A}_3^\mu)\hat{p}_T^\nu,$$

$$\mathcal{E}_1^{\mu\nu} = i\gamma_5\mathcal{A}_2^\mu\hat{p}_T^\nu,$$

$$\mathcal{E}_2^{\mu\nu} = i\gamma_5\mathcal{A}_1^\mu\hat{p}_T^\nu,$$

$$\mathcal{E}_3^{\mu\nu} = -i\gamma_5(\mathcal{A}_6^\mu + \mathcal{A}_4^\mu)\hat{p}_T^\nu,$$

$$\mathcal{E}_4^{\mu\nu} = -i\gamma_5(\mathcal{A}_5^\mu + \mathcal{A}_3^\mu)\hat{p}_T^\nu,$$

$$\mathcal{E}_5^{\mu\nu} = \left(-\frac{2i}{3}\gamma_5\mathcal{A}_4^\mu + \frac{i}{3}\gamma_5\mathcal{A}_6^\mu\right)\hat{p}_T^\nu - \frac{1}{3}\mathcal{S}_1\delta^{\mu\nu},$$

$$\mathcal{E}_6^{\mu\nu} = \left(-\frac{4i}{5}\gamma_5\mathcal{A}_3^\mu + \frac{i}{5}\gamma_5\mathcal{A}_5^\mu\right)\hat{p}_T^\nu - \frac{1}{5}\mathcal{S}_2\delta^{\mu\nu}.$$

The result can be found in Table III. Due to the spin projection by use of the Rarita-Schwinger projector the eigenvalue of $\mathbf{W}^2$ is $\frac{15}{4}$. $\chi^i = \{\chi^{+i}, \chi^{-i}\}$ $(i=1,2,3)$ denotes a two-component vector-spinor which survives the spin-3/2 projection in the rest frame. The Rarita-Schwinger constraints reduce to $\boldsymbol{\sigma\chi} = 0$.

For the decuplet only one s-wave component exists, $\mathcal{D}_1$. Again these covariants exhaust all possible couplings of spin and orbital angular momentum, note that even an orbital angular momentum $l=3$ contributes to a spin-3/2 state, $\mathcal{E}_6$. A contribution of an $l=1$ state with scalar diquark, such as

$$\begin{pmatrix} 0 \\ (\boldsymbol{p\chi}) \end{pmatrix}(\gamma_5 C),$$

is forbidden by the Pauli principle for pure decuplet states, but may admix in the case of broken flavor symmetry.

TABLE III. Classification of the components of the decuplet wave function in terms of eigenstates of $\mathbf{L}^2$ and $\mathbf{S}^2$ in the rest frame of the bound state.

$\psi_{\alpha\beta\gamma}^{10}$ in the rest frame	eigenvalue $l(l+1)$ of $\mathbf{L}^2$	eigenvalue $s(s+1)$ of $\mathbf{S}^2$
$\mathcal{D}_1 u_\mu (\gamma^\mu C) = \begin{pmatrix} \chi^i \\ 0 \end{pmatrix} (\gamma^i C)$	0	$\frac{15}{4}$
$\mathcal{D}_2^{\mu\nu} u_\nu (\gamma^\mu C) = \begin{pmatrix} 0 \\ \frac{1}{p}((\boldsymbol{\sigma p})\chi^i - \frac{2}{3}\sigma^i(\boldsymbol{p\chi})) \end{pmatrix} (\gamma^i C)$	2	$\frac{15}{4}$
$\mathcal{E}_1^{\mu\nu} u_\nu (\gamma^\mu C) = i\hat{P}^0 \begin{pmatrix} \frac{1}{p}(\boldsymbol{p\chi}) \\ 0 \end{pmatrix} (\gamma^4 C)$	2	$\frac{3}{4}$
$\mathcal{E}_2^{\mu\nu} u_\nu (\gamma^\mu C) = i\hat{P}^0 \begin{pmatrix} 0 \\ (\boldsymbol{\sigma\hat{p}})(\boldsymbol{\hat{p}\chi}) \end{pmatrix} (\gamma^4 C)$	6	$\frac{3}{4}$
$\mathcal{E}_3^{\mu\nu} u_\nu (\gamma^\mu C) = \begin{pmatrix} \sigma^i(\boldsymbol{\sigma\hat{p}})(\boldsymbol{\hat{p}\chi}) \\ 0 \end{pmatrix} (\gamma^i C)$	6	$\frac{3}{4}$
$\mathcal{E}_4^{\mu\nu} u_\nu (\gamma^\mu C) = \begin{pmatrix} 0 \\ \frac{1}{p}\sigma^i(\boldsymbol{p\chi}) \end{pmatrix} (\gamma^i C)$	2	$\frac{3}{4}$
$\mathcal{E}_5^{\mu\nu} u_\nu (\gamma^\mu C) = \begin{pmatrix} \hat{p}^i(\boldsymbol{\hat{p}\chi}) - \frac{1}{3}[\chi^i + \sigma^i(\boldsymbol{\sigma\hat{p}})(\boldsymbol{\hat{p}\chi})] \\ 0 \end{pmatrix} (\gamma^i C)$	6	$\frac{15}{4}$
$\mathcal{E}_6^{\mu\nu} u_\nu (\gamma^\mu C) = \begin{pmatrix} 0 \\ \frac{1}{p}(p^i(\boldsymbol{\sigma\hat{p}})(\boldsymbol{\hat{p}\chi}) - \frac{1}{5}[\sigma^i(\boldsymbol{p\chi}) + (\boldsymbol{\sigma p})\chi^i]) \end{pmatrix} (\gamma^i C)$	12	$\frac{15}{4}$

IV. LADDER APPROXIMATION TO THE BETHE-SALPETER EQUATION

In our preceding publication [1] we used a momentum routing in the Bethe-Salpeter equation, where the interaction (propagator of the exchanged quark) is manifestly independent of the total momentum P of the baryon, i.e., $q = -p - p'$. A P-independent kernel is desirable for the following reasons. As will be discussed in the next section, it reduces the numerical work when solving the integral equation quite drastically. Furthermore, the canonical normalization condition for the Bethe-Salpeter wave function [42] becomes much more involved when the interaction is P dependent. Therefore, when solving a Bethe-Salpeter equation in the ladder approximation one usually tries to find a momentum routing having this very convenient feature. In our equations, however, where quark and diquark interact through quark exchange, which changes the identity of the particles after each interaction (a diquark becomes a quark and a quark becomes a diquark after the quark exchange), demanding a P-independent interaction defines a "modified ladder approximation" with results deviating from other momentum routings. Note that this problem does not occur in the Bethe-Salpeter approach if the interaction, e.g., meson exchange in

the two nucleon system or gluon exchange between quark and antiquark, does not change the identity of the constituents. Almost all Bethe-Salpeter equations treated in the literature are of this kind. For a comprehensive review of the existing Bethe-Salpeter literature see Ref. [43]. In order to clarify the ambiguity arising in the diquark-quark Bethe-Salpeter equation, which came up during our investigations, we discuss here two possible momentum routings and in Sec. VI and Appendix the corresponding variations of the results.

For sake of clarity of this discussion we temporarily restrict ourselves to the part of the octet equation which involves only scalar diquarks, i.e., Eq. (3.1) with $g_a = 0$. Furthermore, it is more transparent to work with the Bethe-Salpeter equation which involves the vertex function [see Eq. (3.19)]:

$$\Phi_8(p;P) = -|g_s|^2 \int \frac{d^4p'}{(2\pi)^4} \gamma_5 \widetilde{S}$$
$$\times (-q)\gamma_5 S(p_a')D(p_b')\Phi_8(p';P). \quad (4.1)$$

Repeating the procedure discussed in Sec. III A for the vertex instead of the wave function leads to an *Ansatz* [30,1]
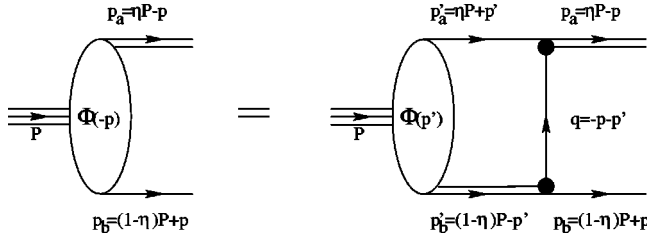
FIG. 1. Momentum routing defining the modified ladder approximation.

FIG. 2. Momentum routing defining the direct ladder approximation.

$$\Phi_8(p;P) = \begin{pmatrix} \mathbf{1}\hat{S}_1(p,z) & 0 \\ \dfrac{1}{p}(\boldsymbol{\sigma}\boldsymbol{p})\hat{S}_2(p,z) & 0 \end{pmatrix}. \qquad (4.2)$$

Note that in the lower component of this spinorlike object the spin is orientated along the spatial part of the relative momentum. In the Bethe-Salpeter equation (4.1) the momentum of the constituent quark is given by $p_a' = p' + \eta P$, and the momentum of the scalar diquark by $p_b' = -p' + (1-\eta)P$. P denotes the total momentum of the nucleon and p the relative momentum between quark and diquark. The Mandelstam parameter η describes how P is partitioned to quark and diquark. The fact that the eigenvalues of the Bethe-Salpeter equation are independent of η is a direct consequence of Lorentz covariance.

If the momentum of the exchanged quark is chosen as $q = -p - p'$, the interaction kernel is by construction independent of the total momentum. Since the quark exchange transforms a quark to a diquark and vice versa, after the interaction, the relative momentum between these particles becomes $(1-\eta)p_a - \eta p_b = -p$, see Fig. 1 for this momentum routing. We now demand $\Phi_8(-p;P) = \Phi_8(\boldsymbol{p},-z,P)$, i.e., the orientation of the nucleon spin should not depend on the orientation of p as required by the Dirac decomposition before projection onto positive energies. Then the vertex function appearing on the left-hand side in Eq. (4.1) reads

$$\Phi_8(p;P) = \begin{pmatrix} \mathbf{1}\hat{S}_1(p,-z) & 0 \\ \dfrac{1}{p}(\boldsymbol{\sigma}\boldsymbol{p})\hat{S}_2(p,-z) & 0 \end{pmatrix}. \qquad (4.3)$$

The definition of the momentum q together with Eq. (4.3) is what we call the "modified ladder approximation" which leads to satisfying results for various nucleon form factors in the weak binding regime, as can be seen in Ref. [1]. Using such a prescription we have been able to reproduce the results of Ref. [30].

Another possible momentum routing allows P to flow through the quark exchange, $q = -p - p' + (1-2\eta)P$, see Fig. 2. When not taking into account that the quark and diquark change their role after exchanging a quark, that means attributing the index a to the quark and index b to the diquark, the relative momentum after the interaction is given by p. Correspondingly, the vertex function on the left-hand side in Eq. (4.1) is denoted by
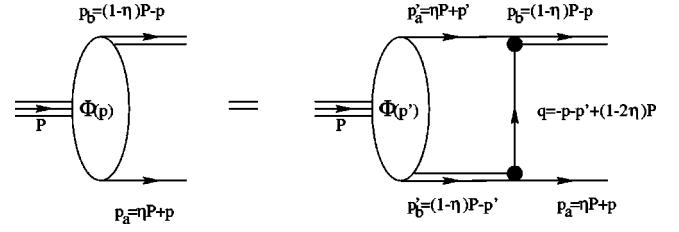
$$\Phi_8(p;P) = \begin{pmatrix} \mathbf{1}\hat{S}_1(p,z) & 0 \\ \dfrac{1}{p}(\boldsymbol{\sigma}\boldsymbol{p}')\,\hat{S}_2(p,z) & 0 \end{pmatrix}. \qquad (4.4)$$

We name this the "direct ladder approach." Although one might expect that both choices of the momentum routing lead to the same physical results, we found that this is actually not the case. In the next sections and Appendix B we report on calculations using both momentum routings, see also Ref. [44] for further results obtained in the direct ladder approach. We found that physical results slightly differ for these two choices. We will show, however, that both possibilities are manifestly Lorentz covariant, i.e., the eigenvalues do not depend on the Mandelstam parameter η. Furthermore, for weak binding the eigenvalues almost coincide. Given that the ladder approximation is only reliable for weak binding we conclude that both methods are of similar validity.

Although during this discussion we restricted ourselves for clarity to scalar diquarks and to the Bethe-Salpeter equation involving the vertex function, it can be extended in a straightforward way to the complete equation including the axial-vector diquark channel, the decuplet equation and also to the Eqs. (3.1) and (3.2) involving the wave functions in an obvious way. The reported numerical results are always given for the full problem.

V. NUMERICAL METHOD

For the numerical solutions of the Bethe-Salpeter equations we developed an iterative hybrid algorithm, which allows a very efficient and fast computation. A description of our numerical method will appear in a forthcoming publication which presents this algorithm in all details [40]. Thus we will focus here on the main steps only.

We solve the Bethe-Salpeter equation as a system of equations for the wave function Ψ and the vertex function Φ, see Eqs. (3.1) and (3.2). Both wave and vertex function can be expanded in the rest frame according to Eq. (3.11) and (3.18). Although there are 10 equations for the eight octet functions, stemming from two equations in the scalar diquark channel and 2×4 equations in the axial-vector diquark channel, we confirmed that two of them are redundant. The decuplet system yields 2×12 equations for eight scalar functions due to the tensor character of the wave function which reduce again to eight independent equations. This especially underlines the necessity of including the subdominant amplitudes describing orbital angular momentum to keep the system closed.

We expand the scalar functions (amplitudes) S,A and

D, E defined in Eqs. (3.8) and (3.17) into Chebyshev polynomials of the second kind,

$$Y_i(P;p) = \sum_{n=0}^{\infty} i^n Y_i^n(P^2;p^2) U_n(\hat{P} \cdot \hat{p}), \qquad (5.1)$$

$$\hat{Y}_i(P;p) = \sum_{n=0}^{\infty} i^n \hat{Y}_i^n(P^2;p^2) U_n(\hat{P} \cdot \hat{p}), \qquad (5.2)$$

where amplitudes with a hat, i.e., $\hat{Y}_i$, belong to the vertex function and the ones without a hat to the wave function. Here we use the generic label Y_i according to $Y_i = \{S_1, S_2, \ldots, A_6\}_{octet}$, $\{D_1, D_2, \ldots, E_6\}_{decuplet}$.

Throughout the calculation we work with usual hyperspherical coordinates

$$\begin{pmatrix} p_1' \\ p_2' \\ p_3' \\ p_4' \end{pmatrix} = p' \begin{pmatrix} \sin\psi' \sin\theta' \sin\phi' \\ \sin\psi' \sin\theta' \cos\phi' \\ \sin\psi' \cos\theta' \\ \cos\psi' \end{pmatrix}, \quad z' = \cos\psi' = \hat{P} \cdot \hat{p}'.$$
$$(5.3)$$

We are free to choose the spatial part of the relative momentum p appearing on the left-hand side of the Bethe-Salpeter equation (3.1). Without loss of generality, we select $p^\mu = (0,0,p\sqrt{1-z^2}, pz)$.

We expand quark and diquark propagators into Chebyshev polynomials as well and project the Bethe-Salpeter equation onto the Chebyshev moments of the amplitudes, $\hat{Y}_i^m, Y_i^m$. Note that in the chosen Lorentz frame with the relative momentum **p** parallel to the third axis this is especially easy because in this case the amplitudes as given in Eq. (3.11) do not mix. The integration necessary to generate the kernel will be performed in hyperspherical coordinates. The integrations over ϕ' and θ' are done analytically, and the remaining two over z' and z (due to the projection) numerically.

The final equation suitable for iteration or diagonalization reads

$$Y_i^m(p_{l_1}) = -g^2 \sum_{j=1}^{8} \sum_{n=0}^{n_{max}} P_{ij}^{mn}(p_{l_1}) \hat{Y}_j^n(p_{l_1}) \qquad (5.4)$$

$$\hat{Y}_j^n(p_{l_1}) = \sum_{k=1}^{8} \sum_{m=0}^{m_{max}} \int_0^{\infty} dp' \, p'^3 H_{jk}^{nm}(p_{l_1}, p_{l_2}') Y_k^m(p_{l_2}'). \qquad (5.5)$$

Here, P_{ij}^{mn} is the propagator matrix with amplitude indices i, j and Chebyshev moment indices m, n and $H_{jk}^{nm}(p, p')$ is the matrix of the quark exchange kernel given on a momentum grid (p_{l_1}, p_{l_2}') with respective amplitude indices j, k and Chebyshev moment indices n, m. The sum over amplitude indices runs from 1 to 8 for both octet and decuplet. m_{max} and n_{max} denote the highest Chebyshev polynomial considered in the expansion of the vertex and the wave function amplitudes, respectively. The kernel includes also the flavor factors and the ratio g_a/g_s (for spin-1/2 baryons). It is only in the modified ladder approximation that the integral kernel does not include an explicit dependence on the bound state mass M for all values of η, which makes a fast determination of M for given couplings feasible. We refer to g as the

TABLE IV. Octet Bethe-Salpeter equation-eigenvalues g_s for various m_{max} and n_{max}, the maximum Chebyshev momenta of vertex and wave function. Parameters: $m_q = m_{0^+} = m_{1^+}$, $M = 1.5 m_q$, $\Lambda = 2 m_q$, $g_a/g_s = 0.5$, $\eta = 0.5$, momentum grid size $n_p = 20$.

	Confining propagators, $d=10$			
	n_{max} 0	1	2	3
m_{max}				
0	9.4362	9.1533	9.1417	9.1420
1	9.7480	9.2277	9.2260	9.2265
2	9.7568	9.2276	9.1992	9.1988
3	9.7568	9.2277	9.1994	9.1990
	Confining propagators, $d=1$			
	n_{max} 0	1	2	3
m_{max}				
0	11.3797	10.9507	10.9544	10.9547
1	11.8555	11.1401	11.1704	11.1711
2	11.8656	11.1503	11.1443	11.1445
3	11.8656	11.1504	11.1444	11.1446

eigenvalue of the Bethe-Salpeter equation which is g_s for spin-1/2 and g_a for spin-3/2 baryons.

In the following we will investigate the convergence properties of the expansion in Chebyshev polynomials. Furthermore, the independence of the eigenvalue from the Mandelstam parameter η will be discussed. The chosen example is the octet equation (3.1) with the axial-vector diquark propagator diagonal in Lorentz indices and a diquark size factor of the monopole type.

For all calculations reported, a momentum mesh size of 20×20 and the inclusion of only zeroth, first, and second Chebyshev moments for both vertex and wave function amplitudes is sufficient for determining the eigenvalue up to 10^{-4} precision (see Table IV). This is also reflected in the magnitudes of the vertex amplitudes $\hat{Y}_i$: Going up one Chebyshev moment suppresses the amplitudes by almost one order of magnitude. The wave function amplitudes Y_i converge somewhat slower, see also Sec. VI C. For a large pole screening factor, $d > 5$, and a weak binding situation the even Chebyshev momenta are more pronounced than the odd ones.

Increasing the coupling constant g_a in the nucleon equation always lowers the eigenvalue, hence the axial-vector diquark enhances binding.

For tree level propagators the choice of the Mandelstam parameter η is limited to the values $\eta \in [1 - \min\{m_{0^+}, m_{1^+}\}/M, m_q/M]$ to avoid singularities in the propagators. This restriction should not apply for confining propagators. To demonstrate this, we choose the extreme case $m_{0^+} = m_{1^+} = 2 m_q$ and the tree level threshold $M = 3 m_q$.[4] Then, tree level propagators limit the choice to $\eta = 1/3$, as opposed to confining propagators. For a small pole

---

[4] For similar choices of quark and diquark masses we calculate the octet and decuplet masses, see Sec. VI. The masses of the decuplet baryons are close to the tree level threshold.
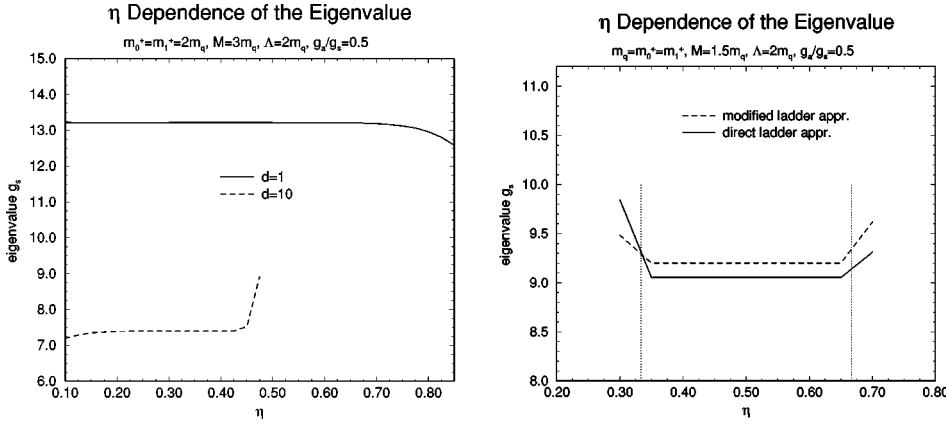
η Dependence of the Eigenvalue

$m_0{}^+ = m_1{}^+ = 2m_q, \; M = 3m_q, \; \Lambda = 2m_q, \; g_a/g_s = 0.5$

η Dependence of the Eigenvalue

$m_q = m_0{}^+ = m_1{}^+, \; M = 1.5m_q, \; \Lambda = 2m_q, \; g_a/g_s = 0.5$

FIG. 3. Eigenvalue vs Mandelstam parameter η, left: two pole screening factors compared, right: modified and direct ladder approach compared. Dotted lines denote the location of the propagator poles.

screening factor $d=1$ we could vary η in a wide range without affecting the eigenvalue, for $d=10$ due to numerical instabilities the invariance region depends on the constituent masses, displayed in Fig. 3 in the left panel. It can be seen that the poles in the tree level propagators are effectively screened although the invariance region for $d=10$ is restricted to 0.2–0.42.

Whereas the latter results were obtained in the modified ladder approximation, the check of η independence for the direct ladder approach requires the total momentum P to appear in the kernel: $q = -p - p' + (1 - 2\eta)P$, which slows down the numerics considerably. In the case of tree level propagators, the right panel of Fig. 3 shows the invariance of the eigenvalue for both momentum routings.

The crucial advantage of using confining propagators can be seen even more clearly in Fig. 4. Here the function $g_s(M)$ decreases rapidly for tree level propagators near threshold while the corresponding function for confining propagators runs smoothly over the ''pseudo''-threshold. We furthermore observe that the even Chebyshev momenta of the Bethe-Salpeter wave functions for tree level propagators close to threshold become squeezed in the low momentum domain while the corresponding odd momenta are suppressed. No such effect is present for the Bethe-Salpeter wave functions obtained with confining propagators.

All the numerical features described also apply to the decuplet equation in the weak binding regime $[M > \frac{3}{4}(m_q + m_0{}^+{}_{,1}{}^+)]$. For lower bound state masses the convergence

Eigenvalue vs. Bound State Mass

$m_q = m_0{}^+ = m_1{}^+, \; \Lambda = 2m_q, \; g_a/g_s = 0.5$

FIG. 4. Eigenvalues vs bound state mass M. Note the absence of threshold effects for confining propagators.

becomes worse and for $M < \frac{1}{2}(m_q + m_0{}^+{}_{,1}{}^+)$ our method failed in finding a real eigenvalue for the coupling g_a. In this mass region an effect well known from the Cutkosky model is visible: two states described by their functions $g_a(M)$ collide and form a complex conjugate pair of eigenvalues [45,46]. This shortcoming of the ladder approximation provides us with an upper limit of the coupling constant g_a for which the approximation is valid. However, the g_a needed to describe the baryon decuplet is well below this critical value.

VI. RESULTS: MASSES AND SELECTED WAVE FUNCTIONS

A. Octet and decuplet masses

In our approach the strange quark constituent mass m_s is the only source of flavor symmetry breaking. Isospin is assumed to be conserved. The equations describing octet and decuplet baryons have been derived under the premises of flavor and spin conservation, i.e., only wave function components with same spin and flavor content couple. The flavor structure of the eight equations describing N, Λ, Σ, Ξ, Δ, Σ^*, Ξ^* and Ω can be found in Appendix A.

In order to limit the number of parameters we assume the scalar and axial-vector diquark masses to be equal. Furthermore, we choose them to be $m_{0^+,1^+}^{fg} = \xi(m_f + m_g)$ where $fg \in \{uu, us, ss\}$ is the flavor content of the diquark. We denote the diquark mass parameter as ξ. Assuming $\xi \in [0,1]$ is obviously natural. With these choices the model has the following parameters: two constituent quark masses $m_u = m_d, m_s$, the pole screening factor d, the diquark size factor Λ, the diquark mass parameter ξ and the couplings g_a, g_s.

We do not try to make a thorough fit onto the baryon masses in our parameter space. Inspired by our results for the form factors of proton and neutron [1], we assume first $d = 10$. This results in only slight modifications of the propagators compared to the tree level ones for spacelike momenta. Furthermore, we choose $\Lambda = 1$ GeV $\approx 2m_u$ and $\xi = 1$ to stay close to calculations of octet and decuplet masses in NJL-diquark-models as done in Refs. [25] and [23]. These authors, however, used just a static approximation to the Bethe-Salpeter equation. Note that this part of our calculation has been done only in modified ladder approximation since we were forced to choose $\eta < 0.4$ (cf. Fig. 3), and
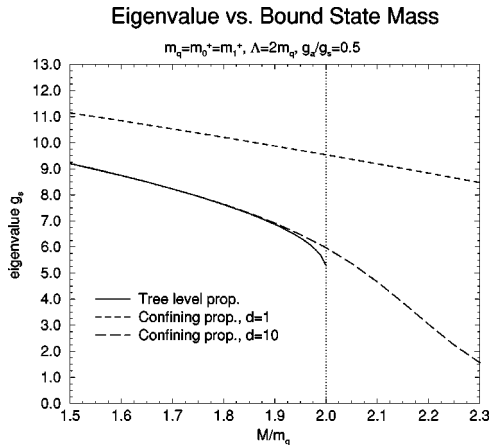
TABLE V. Octet and decuplet masses obtained with the maximum order in Chebyshev polynomials $m_{max}=n_{max}=3$ and momentum grid size $n_p=20$.

| | Expt. | Modified ladder | | Direct ladder |
		I	II	III
d		10	1	1
Λ (GeV)		1	1	1
m_u (GeV)		0.5	0.5	0.5
m_s (GeV)		0.65	0.63	0.63
ξ		1	0.73	0.73
g_a		10.35	10.92	10.05
g_s		9.43	8.06	7.34
M_Λ (GeV)	1.116	1.123	1.130	1.133
M_Σ (GeV)	1.193	1.134	1.137	1.140
M_Ξ (GeV)	1.315	1.307	1.319	1.319
$M_{\Sigma*}$ (GeV)	1.384	1.373	1.372	1.380
$M_{\Xi*}$ (GeV)	1.530	1.545	1.548	1.516
M_Ω (GeV)	1.672	1.692	1.697	1.665
χ^2		0.0028	0.0028	0.0021

solely for $\eta=0.5$ the integral kernel does not depend on the baryon mass in the direct approach, which allows a fast determination of M. We then fix the couplings g_a and g_s by the nucleon and delta mass. The ratio g_a/g_s is quite independent from the ratio M_Δ/m_q and varies weakly with d. Finally we vary just the two constituent quark masses to obtain the other six hyperon masses reasonably close to their experimental values.

Secondly, we explore the case $d=1$ and now additionally allow the diquark mass factor ξ to vary. In Ref. [1] we showed that this strong screening of the propagator poles leads to overestimated nucleon e.m. form factors for high Q^2. In this case we also compare results for the two momentum routings, modified and direct ladder approach. In both calculations η is set to 0.5.

The results are given in Table V. The quality of the results may be read from the quantity

$$\chi^2 = \sum_{i=1}^{6} \frac{(M^i_{\text{theor}} - M^i_{\text{exp}})^2}{(M_{\text{exp}})^2}.$$

Note that the mean deviation of the calculated masses from the experimental ones is of the order of half a per cent or less. Column I shows the results for $d=10$. A remarkable feature is the large constituent quark mass $m_u=500$ MeV, whereas the constituent mass difference between strange and up quark is 160 MeV, a commonly used value. In the following two subsections we will show for this set of parameters the wave function amplitudes for the nucleon and the delta and discuss the contribution of the various components with respect to their orbital angular momentum and exemplify flavor symmetry breaking effects on the wave and vertex function of the Λ hyperon.

Columns II and III show the results for $d=1$ with the other parameters chosen to give baryon masses to the same level of accuracy as before. In this case quark and diquark propagators are strongly modified for spacelike momenta. Quark and diquark "masses" begin to lose their meaning which we usually attach to them. This is reflected in our solutions in a rather small diquark mass parameter which renders constituent quarks and diquarks roughly equal in their masses. The direct and modified ladder approaches give approximately the same results in the latter case.

In all cases the Gell-Mann–Okubo mass formula for the octet is fulfilled with an inaccuracy of less than 0.5%. It should be emphasized that the mass splitting between the octet and decuplet is exclusively provided by the quark exchange with the coupling strengths g_s and g_a and is not due to a heavier axial-vector diquark as assumed in other diquark-quark models, e.g., in Ref. [21].

B. Vertex functions for the Λ-hyperon

The Λ hyperon appears to be of special interest. First, its measured polarization asymmetry in the process $p\gamma\rightarrow K^+\Lambda$ could provide a stringent test for the diquark-quark model. As discussed in Ref. [47], there are only scalar diquarks involved in this process and in the following we will concentrate on the scalar diquark part of the vertex function.

Secondly, broken SU(3)-flavor symmetry induces a component of the total antisymmetric flavor singlet[5] $(1/\sqrt{3})[(su)d+(ud)s+(ds)u]$ into wave and vertex function (see Appendix A).[6] As the flavor singlet is only composed of scalar diquarks and quarks, this generates two additional scalar amplitudes $\hat{S}_{1,\text{singlet}}$ and $\hat{S}_{2,\text{singlet}}$ besides the usual two from the octet Λ state $(1/\sqrt{6})[(su)d-\sqrt{2}(ud)s+(ds)u]$. The vector part of the vertex function remains unchanged in flavor space, $(1/\sqrt{2})([su]^\mu d-[ds]^\mu u)$.

These scalar amplitudes for the vertex function are depicted in Fig. 5 for the parameter set of column I in Table V. The $\hat{S}_{1,\text{singlet}}$ component is suppressed against $\hat{S}_{1,\text{octet}}$ by two orders of magnitude. However, the purely relativistic $\hat{S}_{2,\text{singlet}}$ component is only 5 times smaller than its octet counterpart. Observing that the $\hat{S}_1$ component usually contributes the major part to observables as demonstrated in Ref. [1], we can safely regard the Λ hyperon as an almost pure octet state in flavor space.

C. Wave functions for nucleon and delta

In this subsection we present Bethe-Salpeter wave functions for nucleon and delta, using the parameter set of column I in Table V. They are normalized to $S_1^0(p_1)=1$ (nucleon) or $D_1^0(p_1)=1$ (delta) where p_1 is the smallest point of the momentum mesh. The amplitudes represent the strengths of the $(\mathbf{L}^2, \mathbf{S}^2)$ eigenfunctions given in Sec. III B and are simple linear combinations out of the amplitudes defined in Eqs. (3.8) and (3.17).

---

[5]We denote scalar diquarks, with parentheses, e.g., $(us)=us-su$. Axial-vector diquarks we denote as $[us]=us+su$.

[6]In nonrelativistic quark models with SU(6) symmetry such a component is forbidden by the Pauli principle.
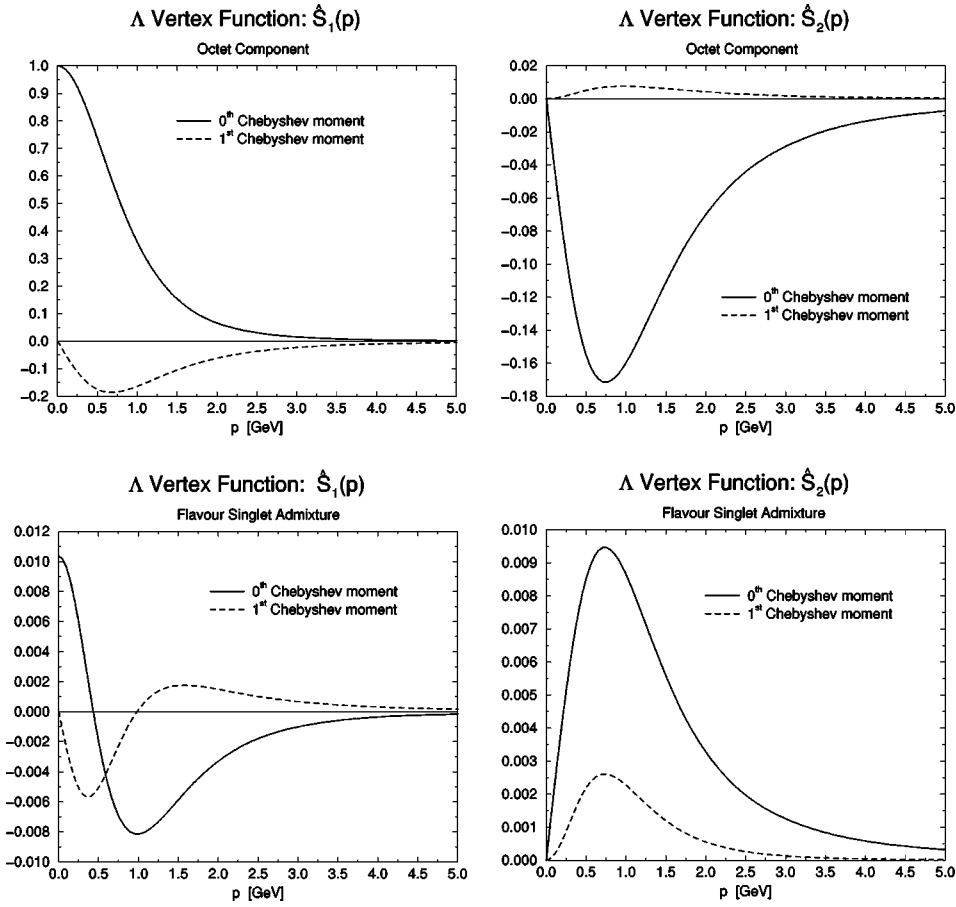
FIG. 5. Scalar amplitudes of the vertex function for the Λ hyperon normalized to $\hat{S}^0_{1,\text{octet}}(p_1) = 1$ with p_1 being the first point on the momentum mesh. The parameters used are $m_u = 0.5$ GeV, $m_s = 0.65$ GeV, $\xi = 1$, $\eta = 0.33$, $d = 10$ and $\Lambda = 1$ GeV.

As already mentioned, the convergence of the wave function amplitudes in terms of Chebyshev polynomials is somewhat slower than for the vertex amplitudes: The second and zeroth Chebyshev moments of the amplitudes differ by less than one order of magnitude. All wave function amplitudes are concentrated to four-momenta $p \leq 0.6$ GeV.

In Fig. 6, the nucleon amplitudes with even orbital angular momentum l appear in the left row: These are the three s waves describing (i) scalar diquark and quark, (ii) and (iii) axial-vector diquark and quark oppositely aligned to give spin 1/2. There are two axial-vector diquark components due to the virtual time component of the latter. The scalar diquark component is the most important but the other s-waves enhance binding by approximately 30%. The fourth ''nonrelativistic'' component is a strongly suppressed d wave with quark and axial-vector diquark aligned to give spin 3/2. The lower components depicted on the right side can be understood as the admixture of negative-energy spinors to the proton wave function and contribute approximately 10% to the binding energy.

The delta amplitudes in Fig. 7 have also been arranged into ''non-relativistic'' (left row) and ''relativistic'' components (right row). As expected, the only s-wave dominates the decomposition, but the relativistic p-wave components, which act repulsively, increase the eigenvalue by approximately 20% and are thus non-negligible. Again the component with the highest orbital angular momentum, $l=3$, is highly suppressed.

No clear effects of flavor symmetry breaking, as in terms of the width in momentum space, can be detected for the

other octet wave functions when compared to the nucleon. For the vertex functions (where the zeroth Chebyshev moment dominates), we observed a limited increase of the width in momentum space with increasing number of s quarks (10% difference between N and Ξ). The width is hereby defined as the absolute value of the relative momentum p where the zeroth Chebyshev moment of an s-wave amplitude reaches half the maximum value.

VII. CONCLUSIONS AND OUTLOOK

In this paper we extended the covariant and confining diquark-quark model of Ref. [1] by including axial-vector diquarks in the description of baryons within the Bethe-Salpeter approach. Thus we were able to calculate the octet baryons masses as well as the decuplet masses and wave functions. We implemented confinement via an effective parametrization of the constituent propagators and demonstrated the existence of bound states beyond the pseudo-threshold.

We decomposed octet and decuplet vertex and wave functions in the Dirac and Lorentz algebra, obtaining eight scalar functions, respectively, which we computed numerically. Two approximations to the Bethe-Salpeter equation were discussed and compared: The direct ladder approximation, and a modified ladder approximation with a special momentum routing leading to a kernel independent of the bound state mass.

In order to fix the parameters of the model preliminarily, we computed the masses of octet and decuplet for broken
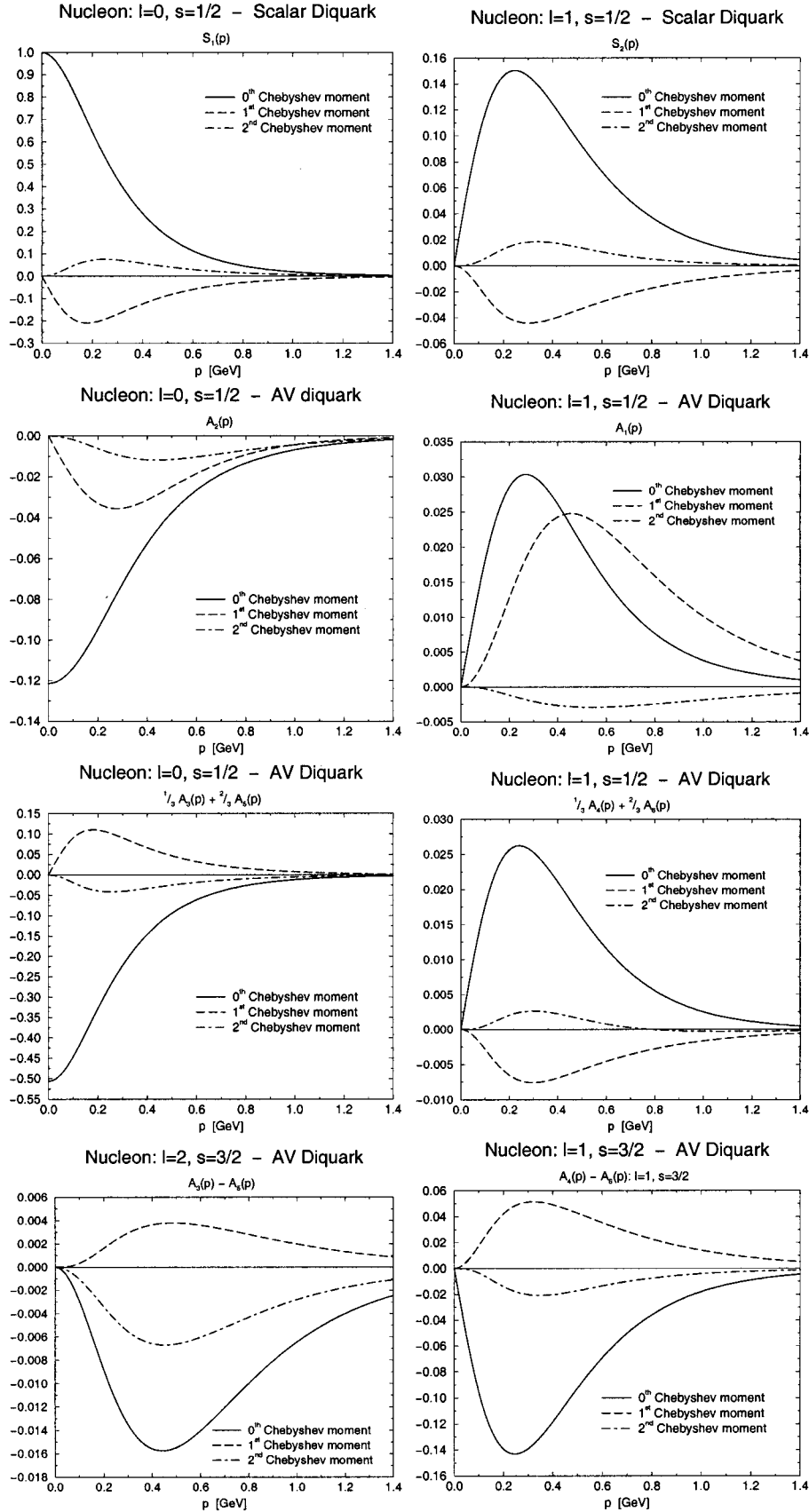
FIG. 6. Scalar and axial vector amplitudes of the nucleon wave function with parameters given by $m_u = 0.5$ GeV, $\xi = 1$, $\eta = 0.33$, $d = 10$, and $\Lambda = 1$ GeV.
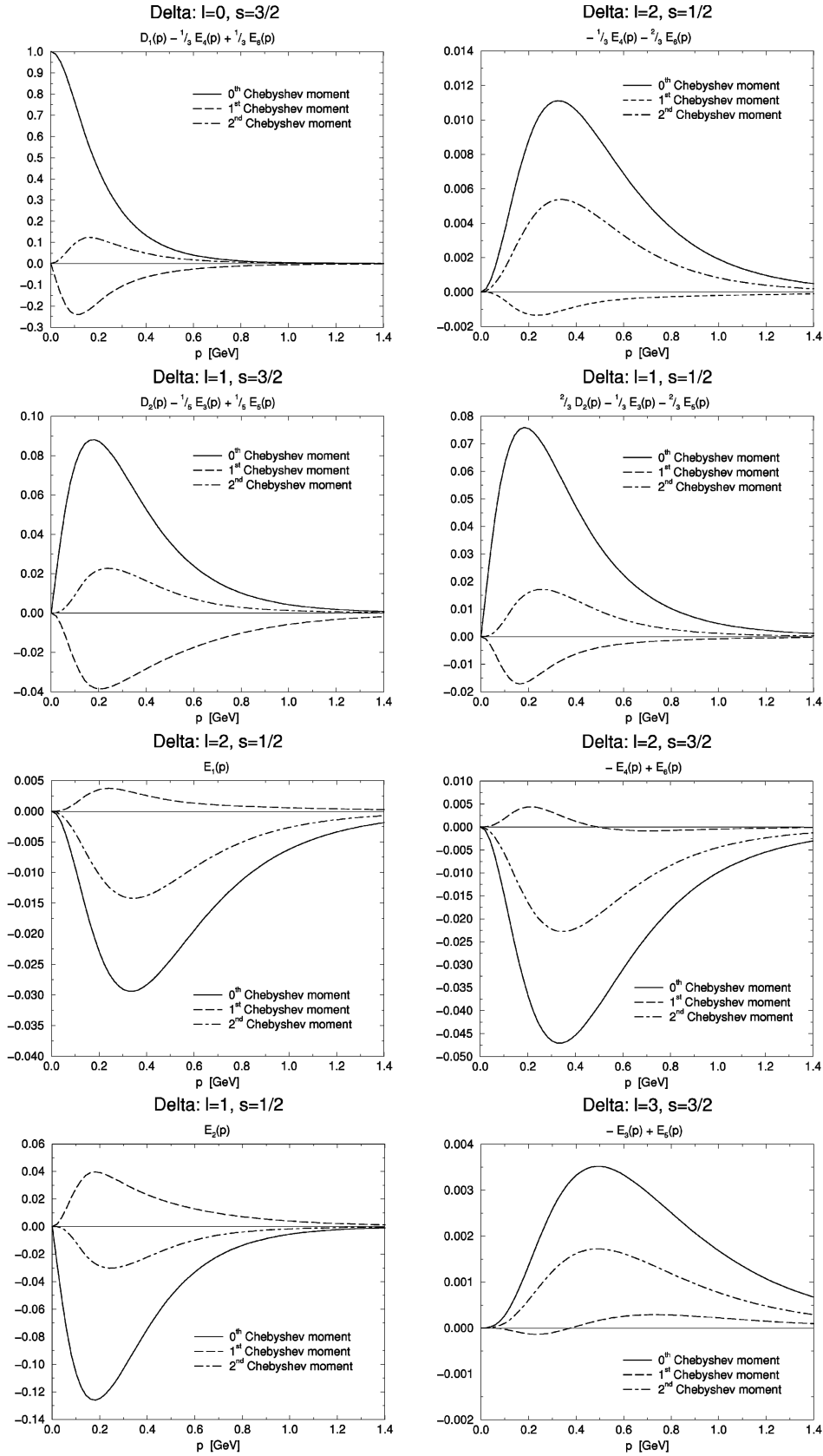
FIG. 7. Axial vector amplitudes of the delta wave function with parameters given by $m_u = 0.5$ GeV, $\xi = 1$, $\eta = 0.33$, $d = 10$, and $\Lambda = 1$ GeV.

SU(3)$_{\text{flavor}}$ with isospin conserved. With the scalar and axial-vector diquark mass assumed to be equal, the octet-decuplet mass splitting is a result of the different effects of the coupling constants in the scalar and axial-vector diquark channel. For a parameter set which fits the octet and decuplet masses well, we computed vertex amplitudes and wave functions for all octet and decuplet baryons. The wave functions for baryons with different strangeness content but the same spin differ mostly due to the different flavor Clebsch-Gordan coefficients, the respective scalar functions being very similar. Therefore we presented only the wave functions for the nucleon and delta out of this data. The decomposition of the wave functions in the rest frame of the bound state in terms of spin and orbital angular momentum eigenstates revealed an s-wave dominance in all ground state baryons stemming from both scalar and axial-vector diquark contributions. The p-wave contributions sneaking in via the lower components of the spinors are of greater importance for decuplet baryons than for octet baryons.

Due to its special role among the other baryons, we investigated the Λ hyperon in more detail and discussed its vertex amplitudes. In our approach, the Λ acquires a small flavor singlet admixture which is absent in SU(6) symmetric nonrelativistic quark models.

This work, together with our preceding paper [1], provides a sound basis for further applications of this approach to baryon phenomenology. The calculated amplitudes which encode the nontrivial information of a baryon as a diquark-quark bound state serve as a necessary input for the calculation of various observables. A calculation of the electromagnetic form factors of the octet and decuplet baryons is hereby the next task. Such an investigation will furthermore help to fix some of the parameters. Our aim is, however, to apply the covariant and confining diquark-quark model to processes, which are far less understood. Especially, the reactions $p\gamma \rightarrow K\Lambda$ and $pp\rightarrow p\Lambda K$, currently measured at ELSA and COSY, respectively, will serve as a stringent test of our approach. Additionally, we plan to get further insight into this picture of baryons by computing structure functions for a spectator model [30] which includes the axial-vector diquark.

APPENDIX A: OCTET AND DECUPLET EQUATIONS

The symmetric and antisymmetric flavor matrices can be written as

$$t_{\mathcal{A}}^a = \{\rho^{a=1\ldots3}\} = \left\{ \begin{pmatrix} 0 & 1 & 0 \\ -1 & 0 & 0 \\ 0 & 0 & 0 \end{pmatrix}, \begin{pmatrix} 0 & 0 & 1 \\ 0 & 0 & 0 \\ -1 & 0 & 0 \end{pmatrix}, \begin{pmatrix} 0 & 0 & 0 \\ 0 & 0 & 1 \\ 0 & -1 & 0 \end{pmatrix} \right\}, \tag{A1}$$

$$t_{\mathcal{S}}^a = \{\rho^{a=4\ldots9}\}$$

$$= \left\{ \begin{pmatrix} \sqrt{2} & 0 & 0 \\ 0 & 0 & 0 \\ 0 & 0 & 0 \end{pmatrix}, \begin{pmatrix} 0 & 0 & 0 \\ 0 & \sqrt{2} & 0 \\ 0 & 0 & 0 \end{pmatrix}, \begin{pmatrix} 0 & 0 & 0 \\ 0 & 0 & 0 \\ 0 & 0 & \sqrt{2} \end{pmatrix}, \begin{pmatrix} 0 & 1 & 0 \\ 1 & 0 & 0 \\ 0 & 0 & 0 \end{pmatrix}, \begin{pmatrix} 0 & 0 & 1 \\ 0 & 0 & 0 \\ 1 & 0 & 0 \end{pmatrix}, \begin{pmatrix} 0 & 0 & 0 \\ 0 & 0 & 1 \\ 0 & 1 & 0 \end{pmatrix} \right\}. \tag{A2}$$

By these conventions flavor antisymmetric diquarks are $(ud):=ud-du$, etc., and flavor symmetric diquarks $\sqrt{2}uu, [ud]:=ud+du$, etc. The flavor wave functions of octet and decuplet states do not decouple once the s quark breaks the symmetry. The Bethe-Salpeter equation (3.1) still describes nucleons (isospin is assumed to be conserved), and Eq. (3.2) still refers to Δ and Ω which possess only single-component flavor wave functions $[uu]^{\mu\rho}u$, respectively, $[ss]^{\mu\rho}s$.

We use the following abbreviations to give short-hand Bethe-Salpeter equations for the remaining baryons:

$(ab)c$ and $[ab]^\mu c$:   octet flavor wave functions with diquark flavor content ab and spectator quark of flavor c;

$[ab]^{\mu\rho}c$:   decuplet flavor wave functions;

S_a: quark propagator of the spectator quark a;

$D_{(ab)}$ and $D_{[ab]}^{\mu\mu'}$:   scalar and axial-vector diquark propagator;

$K_a^{\rho\lambda} = \int [d^4p'/(2\pi)^4]\gamma^\rho \tilde{S}_a(-q)\gamma^\lambda$ $(\rho,\lambda=1\ldots5)$:   exchange kernel for quark flavor a, see Eq. (3.3) for the definition of $\tilde{S}$.

Of course, in contrast to Eqs. (2.3)–(2.5), different masses corresponding to the flavor content of the quark and diquark are used in the numerators and denominators of the propagators.

For octet states each flavor wave function with scalar diquarks is to be expanded in Dirac space according to Eq. (3.11) with only the scalar amplitudes S_1 and S_2 and each one with axial-vector diquarks according to the same equation with the six vector amplitudes $A_1 \ldots A_6$. For decuplet states only flavor wave functions with axial-vector diquarks are considered, they have to be expanded as indicated in Eq. (3.18).

The Bethe-Salpeter equation for Ξ baryons now reads

$$
\begin{pmatrix} (us)s \\ [us]^\mu s \\ [ss]^\mu u \end{pmatrix} = -g_s^2 \begin{pmatrix} S_s D_{(us)} & 0 & 0 \\ 0 & S_s D_{[us]}^{\mu\mu'} & 0 \\ 0 & 0 & S_u D_{[ss]}^{\mu\mu'} \end{pmatrix} \begin{pmatrix} K_u^{5,5} & -\dfrac{g_a}{g_s} K_u^{\nu,5} & \sqrt{2}\dfrac{g_a}{g_s} K_s^{\nu,5} \\ -\dfrac{g_a}{g_s} K_u^{5,\mu'} & \dfrac{g_a^2}{g_s^2} K_u^{\nu\mu'} & \sqrt{2}\dfrac{g_a^2}{g_s^2} K_s^{\nu\mu'} \\ \sqrt{2}\dfrac{g_a}{g_s} K_s^{5,\mu'} & \sqrt{2}\dfrac{g_a^2}{g_s^2} K_s^{\nu\mu'} & 0 \end{pmatrix} \begin{pmatrix} (us)s \\ [us]^\nu s \\ [ss]^\nu u \end{pmatrix}. \tag{A3}
$$

By interchanging $s \leftrightarrow u$ one obtains immediately the equation for Σ baryons.

Broken SU(3) couples the symmetric Λ and the flavor singlet. We introduce the flavor wave functions $F_1 = (1/\sqrt{2})[(us)d-(ds)u]$, $F_2=(ud)s$ and $\Lambda^\mu=(1/\sqrt{2})([us]^\mu d-[ds]^\mu u)$ and the equation for the physical Λ reads

$$
\begin{pmatrix} F_1 \\ F_2 \\ \Lambda^\mu \end{pmatrix} = -g_s^2 \begin{pmatrix} S_u D_{(us)} & 0 & 0 \\ 0 & S_s D_{(ud)} & 0 \\ 0 & 0 & S_u D_{[us]}^{\mu\mu'} \end{pmatrix} \begin{pmatrix} -K_s^{5,5} & \sqrt{2} K_u^{5,5} & -\dfrac{g_a}{g_s} K_s^{\nu,5} \\ \sqrt{2} K_u^{5,5} & 0 & -\sqrt{2}\dfrac{g_a}{g_s} K_u^{\nu,5} \\ -\dfrac{g_a}{g_s} K_s^{5,\mu'} & -\sqrt{2}\dfrac{g_a}{g_s} K_u^{5,\mu'} & -\dfrac{g_a^2}{g_s^2} K_s^{\nu\mu'} \end{pmatrix} \begin{pmatrix} (us)s \\ [us]^\nu s \\ [ss]^\nu u \end{pmatrix}. \tag{A4}
$$

The Ξ^* baryons belonging to the decuplet are described by the equation

$$
\begin{pmatrix} [us]^{\mu\rho}s \\ [ss]^{\mu\rho}u \end{pmatrix} = -g_a^2 \begin{pmatrix} S_s D_{[us]}^{\mu\mu'} & 0 \\ 0 & S_u D_{[ss]}^{\mu\mu'} \end{pmatrix} \begin{pmatrix} K_u^{\nu\mu'} & \sqrt{2} K_s^{\nu\mu'} \\ \sqrt{2} K_s^{\nu\mu'} & 0 \end{pmatrix} \begin{pmatrix} [us]^{\nu\rho}s \\ [ss]^{\nu\rho}u \end{pmatrix}. \tag{A5}
$$

As before the equation for the Σ^* baryons may be obtained by interchanging $s \leftrightarrow u$. Note that we neglected contributions from a state with scalar diquark (us).
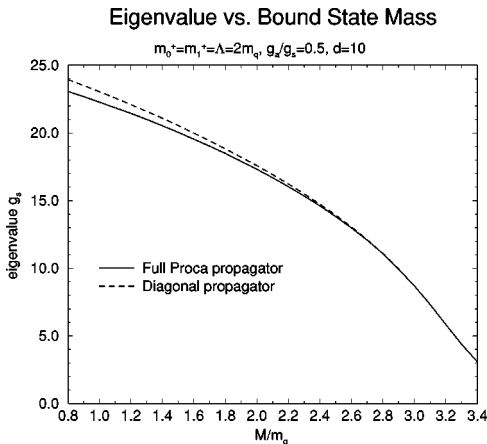

FIG. 8. Eigenvalues vs bound state mass M in the octet equation, and the axial-vector diquark propagator with and without diagonal approximation.
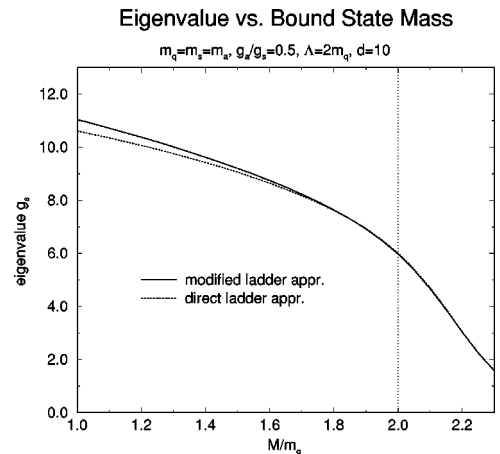

FIG. 9. Eigenvalues vs bound state mass M for direct and modified ladder approximations.
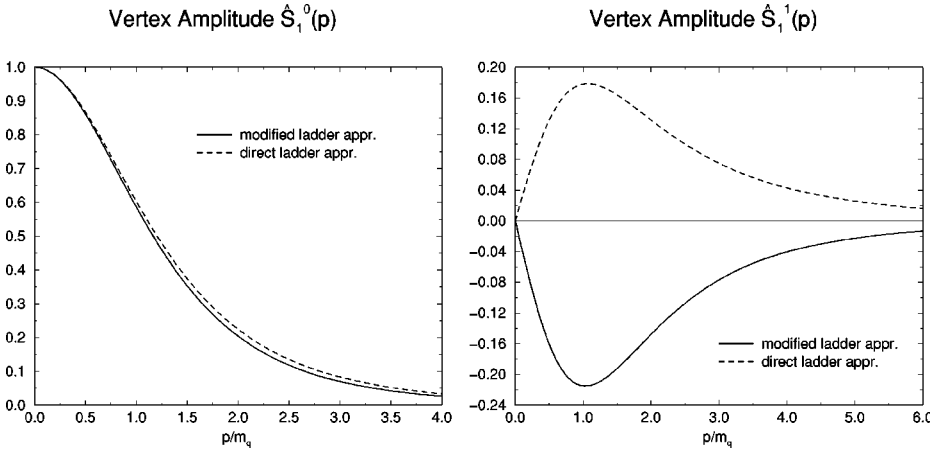
FIG. 10. Zeroth (left) and first (right) Chebyshev moment of the vertex amplitude $\hat{S}_1$. The parameters are $m_q = m_{0^+} = m_{1^+}$, $M = 1.9 m_q$, $\Lambda = 2 m_q$, $g_a/g_s = 0.5$ and $d = 10$.

APPENDIX B: SOLUTIONS WITH PROCA PROPAGATOR FOR AXIAL-VECTOR DIQUARKS

In order to study the influence of the full Proca propagator on vertex functions of spin-1/2 baryons and the corresponding eigenvalues we are forced to use a diquark size factor of the dipole type, writing instead of Eq. (3.3)

$$S(q) \rightarrow \tilde{S}(q) = S(q) \left(\frac{\Lambda^2}{q^2 + \Lambda^2} \right)^2 \qquad \text{(B1)}$$

to regularize the equation which has no stable solution otherwise.

In Fig. 8 we compare the eigenvalues as a function of M for both the Proca propagator and its diagonal approximation. Even in regions of moderate binding the eigenvalues do not differ by more than 2% which makes the approximation of the diagonal propagator in computing the masses a reliable one. While the vertex functions are essentially the same for both choices of the axial-vector diquark propagator, the A_1 components of the Bethe-Salpeter wave function differ by approximately a factor of 10.

APPENDIX C: DIRECT VS MODIFIED LADDER APPROXIMATION

In Fig. 9 we display for a representative parameter set the eigenvalues obtained in direct and modified ladder approximations. One clearly sees that for bound state masses approximately equal to the sum of the constituent masses the eigenvalues are almost identical, and even for strongly bound states the deviation is small.

However, larger deviations occur in the vertex functions. Figure 10 shows zeroth and first Chebyshev moments of $\hat{S}_1$ for modified and direct ladder approximation. Whereas $\hat{S}_1^0$ hardly differs for the two approaches, $\hat{S}_1^1$ receives a sign flip when switching between the two approaches. This occurs for almost all amplitudes in odd Chebyshev moments. When considering the Bethe-Salpeter equation for nucleons with $g_a = 0$, the different sign in $\hat{S}_1^1$ causes the electric form factor of the neutron to change. Isospin breaking effects are also different: The neutron-proton mass difference is in the direct approach bigger than the constituent quark mass difference $m_d - m_u$ whereas in the modified ladder approximation it assumes values of approximately $0.7(m_d - m_u)$ [48].

[1] G. Hellstern, R. Alkofer, M. Oettel, and H. Reinhardt, Nucl. Phys. **A627**, 679 (1997).

[2] M. Anselmino, E. Predazzi, S. Ekelin, S. Fredriksson, and D. B. Lichtenberg, Rev. Mod. Phys. **65**, 1199 (1993).

[3] *Proceedings of the Conference Diquark 3*, Torino, 1996, edited by M. Anselmino and E. Predazzi (World Scientific, Singapore, 1997).

[4] M. Heß, F. Karsch, E. Laermann, and I. Wetzorke, hep-lat/9804023.

[5] T. H. R. Skyrme, Proc. R. Soc. London, Ser. A **260**, 127 (1961), for a recent review of the Skyrme model in flavor SU(3), see H. Weigel, Int. J. Mod. Phys. A **11**, 2419 (1996).

[6] G. Karl and E. Obryk, Nucl. Phys. **B8**, 609 (1968).

[7] D. Faiman and A. W. Hendry, Phys. Rev. **173**, 1720 (1968).

[8] R. P. Feynman, M. Kislinger, and F. Ravndal, Phys. Rev. D **3**, 2706 (1971).

[9] A. Chodos and C. Thorn, Phys. Rev. D **12**, 2733 (1975).

[10] P. Hasenfratz and J. Kuti, Phys. Rep. **40**, 75 (1978).

[11] M. Rho, Phys. Rep. **240**, 1 (1994).

[12] Y. Nambu and G. Jona-Lasinio, Phys. Rev. **122**, 345 (1961).

[13] Y. Nambu and G. Jona-Lasinio, Phys. Rev. **124**, 246 (1961).

[14] T. Hatsuda and T. Kunihiro, Phys. Rep. **247**, 221 (1994).

[15] D. Ebert, H. Reinhardt, and M. K. Volkov, Prog. Part. Nucl. Phys. **33**, 1 (1994).

[16] R. Alkofer and H. Reinhardt, *Chiral Quark Dynamics* (Springer-Verlag, Berlin, 1995).

[17] H. Reinhardt and R. Wünsch, Phys. Lett. B **215**, 577 (1988).

[18] R. Alkofer, H. Reinhardt, and H. Weigel, Phys. Rep. **265**, 139 (1996).

[19] C. V. Christov *et al.*, Prog. Part. Nucl. Phys. **37**, 1 (1996).

[20] H. Reinhardt, Phys. Lett. B **244**, 316 (1990).

[21] U. Vogl and W. Weise, Prog. Part. Nucl. Phys. **27**, 195 (1991).

[22] A. Buck, R. Alkofer, and H. Reinhardt, Phys. Lett. B **286**, 29 (1992).

[23] A. Buck and H. Reinhardt, Phys. Lett. B **356**, 168 (1995).

[24] S. Huang and J. Tjon, Phys. Rev. C **49**, 1702 (1994).

[25] C. Hanhart and S. Krewald, Phys. Lett. B **344**, 55 (1995).

[26] N. Ishii, W. Bentz, and K. Yazaki, Phys. Lett. B **301**, 165 (1993); **318**, 26 (1993); Nucl. Phys. **A587**, 617 (1995).

[27] U. Zückert, R. Alkofer, H. Weigel, and H. Reinhardt, Phys. Rev. C **55**, 2030 (1997).

[28] R. T. Cahill, Nucl. Phys. **A543**, 63 (1992).

[29] H. Meyer, Phys. Lett. B **337**, 37 (1994).

[30] K. Kusaka, G. Piller, A. W. Thomas, and A. G. Williams, Phys. Rev. D **55**, 5299 (1997).

[31] L. Faddeev, Sov. Phys. JETP **12**, 1014 (1961).

[32] V. Keiner, Phys. Rev. C **54**, 3232 (1996); Z. Phys. A **359**, 91 (1997).

[33] C. D. Roberts and A. G. Williams, Prog. Part. Nucl. Phys. **33**, 477 (1994).

[34] R. T. Cahill, C. D. Roberts, and J. Praschifka, Phys. Rev. D **36**, 2804 (1987).

[35] V. Thorsson and I. Zahed, Phys. Rev. D **41**, 3442 (1990).

[36] C. Weiss, A. Buck, R. Alkofer, and H. Reinhardt, Phys. Lett. B **312**, 6 (1993).

[37] H. J. Munczek and A. M. Nemirovsky, Phys. Rev. D **28**, 181 (1983).

[38] A. Bender, C. D. Roberts, and L. v. Smekal, Phys. Lett. B **380**, 7 (1996).

[39] G. Hellstern, R. Alkofer, and H. Reinhardt, Nucl. Phys. **A625**, 697 (1997).

[40] M. Oettel, G. Hellstern, and R. Alkofer, ''An Iterative Solution to Fermion-Boson-Bethe-Salpeter Equations'' (in preparation).

[41] A. B. Henriques, B. H. Kellet, and R. G. Moorhouse, Ann. Phys. (N.Y.) **93**, 125 (1975).

[42] C. Itzykson and J. B. Zuber, *Quantum Field Theory* (McGraw-Hill, New York, 1985).

[43] N. Nakanishi, Prog. Theor. Phys. Suppl. **43**, 1 (1988).

[44] M. A. Pichowsky and L. v. Smekal, ''Quark-Diquark Bound States and the Ward Identity'' (in preparation).

[45] W. B. Kaufmann, Phys. Rev. **187**, 2051 (1969).

[46] S. Ahlig, Diploma thesis, Tübingen University, 1998.

[47] P. Kroll, M. Schürmann, K. Passek, and W. Schweiger, Phys. Rev. D **55**, 4315 (1997).

[48] M. Oettel, Diploma thesis, Tübingen University, 1997.